EurJIC
European Journal of Inorganic Chemistry

Full Papers
doi.org/10.1002/ejic.202100399

Chemistry Europe
European Chemical Societies Publishing

Variation on the π-Acceptor Ligand within a Rh^{I}–N-Heterocyclic Carbene Framework: Divergent Catalytic Outcomes for Phenylacetylene-Methanol Transformations

María Galiana-Cameo,[a] Vincenzo Passarelli,[a] Jesús J. Pérez-Torrente,[a] Andrea Di Giuseppe,*[a, b] and Ricardo Castarlenas*[a]

A series of neutral and cationic rhodium complexes bearing IPr {IPr = 1,3-bis-(2,6-diisopropylphenyl)imidazolin-2-carbene} and π-acceptor ligands are reported. Cationic species $[Rh(\eta^4\text{-cod})(IPr)(NCCH_3)]^+$ and $[Rh(CO)(IPr)(L)_2]^+$ (L = pyridine, CH_3CN) were obtained by chlorido abstraction in suitable complexes, whereas the cod-CO derivative $[Rh(\eta^4\text{-cod})(IPr)(CO)]^+$ was formed by the carbonylation of $[Rh(\eta^4\text{-cod})(IPr)(NCCH_3)]^+$. Alternatively, neutral derivatives of type $RhCl(IPr)(L)_2$ {L = ^{t}BuNC or $P(OMe)_3$} can be accessed from $[Rh(\mu\text{-Cl})(\eta^2\text{-coe})(IPr)]_2$. In addition, the mononuclear species $Rh(CN)(\eta^4\text{-cod})(IPr)$ was prepared by cyanide-chlorido anion exchange, which after carbonylation afforded the unusual trinuclear compound $[Rh\{1\kappa C,2\kappa N\text{-(CN)}\}(CO)(IPr)]_3$. Divergent catalytic outcomes in the phenylacetylene-methanol transformations have been observed. Thus, enol ethers, arisen from hydroalkoxylation of the alkyne, were obtained with neutral Rh–CO catalyst precursors whereas dienol ethers were formed with cationic catalysts. Variable amounts of alkyne dimerization, cyclotrimerization or polymerization products were obtained in the absence of a strong π-acceptor ligand on the catalyst.

Introduction

The detailed study of the coordination properties of organometallic catalysts stands out at the central core of synthetic efficiency. A complex interplay between the stereoelectronic influence exerted by the ligands and the availability of vacant sites in the metal coordination sphere accounts for a successful catalytic performance. Commonly, each elementary step of a catalytic cycle (oxidative addition, reductive elimination…) can be enhanced by opposite electronic effects. Hence, the concurrence of stronger σ-donor with powerful π-acceptor ligands could play a synergic role over the whole catalytic process. Moreover, strongly bonded ligands may prevent undesired reactivity of highly unsaturated catalytic active species. In this context, N-Heterocyclic carbenes (NHCs)[1] and carbon monoxide[2] are a typical pair of donor-acceptor collaborative ligands. The benefits of this association redound not only to the stability of metal complexes,[3] but also to the enhancement of the catalytic activity.[4] Particularly for rhodium-based examples, the preparation of $RhCl(NHC)(CO)_2$ species is now established as a routine method for the analysis of the electronic properties of almost any newly synthesized NHC-type architecture.[5] Regarding catalytic applications, hydroformylation is prevalent for the Rh–NHC–CO systems, certainly prompted by the involvement of carbon monoxide as reagent.[6] Nevertheless, interesting carbon-carbon and carbon-heteroatom coupling reactions have also been described (Figure 1).[7] Particularly remarkable are the contributions by the research groups led by Profs. Messerle[7f] and Bera[7h] dealing with the preparation of enol ethers by alkyne hydroalkoxylation. Other π-acceptor ligands alternative to CO include the neutral isocyanide[8] or phosphite[9] moieties or the cyanide[10] anion.

In the last decade, our research interests have been focused on the study of catalytic applications of Rh–NHC complexes.[11] We have developed efficient promoters for an array of transformations ranging from β-selective H/D exchange of α-olefins, alkyne hydrofunctionalizations (hydrothiolation, hydrophosphination or head-to-tail selective dimerization), or carbon-carbon and carbon-nitrogen couplings via C–H activation. The detailed study of the coordination chemistry of Rh–NHC-based complexes has enabled the evolution of the parent catalytic systems.[12] Particularly, the combined stereoelectronic effects of the tandem NHC–CO have been fundamental for the selective formation of *gem*-vinyl sulfides in alkyne hydrothiolation processes due to the stabilization of Rh^{I} catalytic active species.[7k] Moreover, systematic studies on the coordination of small molecules to neutral and cationic Rh^{I}-NHC scaffolds have been carried out by James,[13] Crudden,[14] and our research

[a] M. Galiana-Cameo, Dr. V. Passarelli, Prof. J. J. Pérez-Torrente, Dr. A. Di Giuseppe, Dr. R. Castarlenas
Departamento de Química Inorgánica-Instituto de Síntesis Química y Catálisis Homogénea (ISQCH),
Universidad de Zaragoza-CSIC
C/Pedro Cerbuna 12, CP 50009, Zaragoza, Spain
E-mail: andrea.digiuseppe@univaq.it
rcastar@unizar.es
http://www.isqch.unizar-csic.es/ISQCHportal/grupos.do?id=29
[b] Dr. A. Di Giuseppe
Dipartimento di Scienze Fisiche e Chimiche, Università dell'Aquila
Via Vetoio, 67100 Coppito (AQ), Italy

Supporting information for this article is available on the WWW under https://doi.org/10.1002/ejic.202100399

Part of the "RSEQ-GEQO Prize Winners" Special Collection.

Full Papers
doi.org/10.1002/ejic.202100399

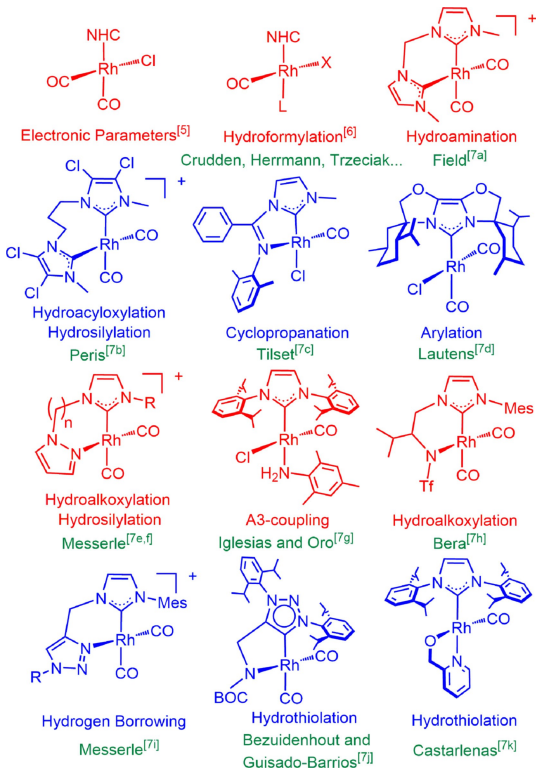

Figure 1. Representative catalytic applications of Rh–NHC–CO complexes.

group.[15] Now, herein we disclose the preparation of a set of Rh^{I} complexes bearing a powerful σ-electron-donor NHC and a variety of π-acceptor ligands, and its impact on phenylacetylene-methanol catalytic transformations.

Results and Discussion

Synthesis of cationic complexes $[Rh(IPr)(L)_2L']^+$ and $[Rh(\eta^4\text{-cod})(IPr)L]^+$

The new cationic complexes bearing π-acceptor ligands have been prepared from the organometallic precursors $RhCl(\eta^4\text{-cod})(IPr)$[13a] (**1**), $RhCl(CO)_2(IPr)$[13c] (**2**), and $[Rh(\mu\text{-Cl})(\eta^2\text{-coe})(IPr)]_2$[13b] (**3**) {IPr = 1,3-bis-(2,6-diisopropylphenyl)imidazolin-2-carbene; cod = 1,5-cyclooctadiene, coe = *cis*-cyclooctene}. Treatment of **2** with $TlPF_6$ in coordinating solvents afforded cationic complexes of type $[Rh(CO)(IPr)(L)_2][PF_6]$ (**4**, L = py; **5**, L = CH_3CN), as a result of the removal of the chlorido ligand and the replacement of the carbonyl moiety located *trans* to the carbene with a solvent molecule (Scheme 1). The use of $AgPF_6$ resulted in the formation of other unidentified complexes as impurities. The bis-CO complex $[Rh(CO)_2(IPr)(NCCH_3)][PF_6]$ (**6**) was obtained by bubbling carbon monoxide through a CH_2Cl_2 solution of **5** at room temperature. The carbonylation of **5** is reversible, thus, addition of CH_3CN to a solution of **6** in CH_2Cl_2 (1:1) resulted in the recovery of bis-acetonitrile complex **5**. The complexes were obtained in 65–80% yield as yellow solids

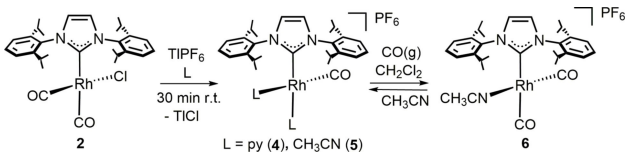

Scheme 1. Preparation of cationic solvento-complexes **4**–**6**.

which are stable in the open air for months. Decoordination of a CO molecule located *trans* to a powerful electron-donor NHC ligand is not unexpected.[15b,16] In fact, this behavior has been recently exploited in the biomedical applications of CO-release molecules (CORMs).[17] Moreover, although pyridine is an ubiquitous ligand in coordination chemistry, a mutually pyridine-NHC *cis* disposition is uncommon in square-planar d^8 structures[15b,18] and the concomitant presence of two molecules of pyridine is unprecedented in Rh^{I}-NHC chemistry.[19]

The crystal structure of **4** and **5** (Figure 2) shows a distorted square planar environment at the metal centre with a *cis* disposition of the NHC and CO ligands [**4**, C1-Rh–C42 87.98(12)°; **5**, C1-Rh1-C36 90.96(16)°], pyridine or acetonitrile occupying the remaining coordination sites [**4**, N30-Rh1-N36 84.22(9)°; **5**, N30-Rh1-N33 85.66(13)°]. Remarkably, the rhodium-nitrogen bond lengths are indicative of a similar *trans* influence of the CO and the NHC ligands [**4**, Rh1-N30 2.110(2) Å, Rh1-N36 2.123(2) Å; **5**, Rh1-N30 2.055(4) Å, Rh1-N33 2.072(3) Å]. Also, it is worth a mention that the steric hindrance of the NHC ligand forces the *cis* pyridine (**4**) or acetonitrile (**5**) out of the ideal arrangement with respect to the rhodium-nitrogen bond. As a matter of fact, as for **4** the pitch angle of the pyridine ligand N36-C37-C38-C39-C40-C41 *cis* to C1 (θ 12.0°) is bigger than that calculated for the pyridine ligand N30-C31-C32-C33-C34-C35 *trans* to C1 (θ 5.0°). By the same token, as for **5** the angle Rh1-N33-C34 [170.7(3)°] is smaller than the angle Rh1-N30-C31 [176.4(5)°]. Finally, it should also be noted that the

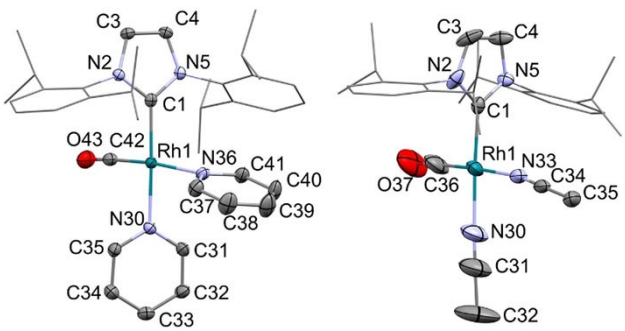

Figure 2. ORTEP view of $[Rh(CO)(IPr)(py)_2]^+$ in **4** (*left*) and $[Rh(CO)(IPr)(CH_3CN)_2]^+$ in **5** (*right*) with ellipsoids at 50% probability. For clarity hydrogen atoms are omitted and a wireframe style is adopted for the 2,5-$(iPr)_2C_6H_3$ moiety of the IPr ligand. Selected bond lengths (Å) and angles (°) are: **4**, Rh1-C42 1.815(3), Rh1-C1 2.010(3), Rh1-N30 2.110(2), Rh1-N36 2.123(2), O43-C42 1.142(4), C1-Rh1-C42 87.98(12), C1-Rh1-N30 177.36(11), C1-Rh1-N36 98.34(10), N30-Rh1-N36 84.22(9); **5**, C1-Rh1 1.997(3), C36-Rh1 1.814(5), N30-Rh1 2.055(4), N33-Rh1 2.072(3), C36-O37 1.143(5), C1-Rh1-C36 90.96(16), C1-Rh1-N33 91.96(11), C1-Rh1-N30 177.28(14), N30-Rh1-N33 85.66(13), Rh1-C31-N30 176.4(5), Rh1-C34-N33 170.7(3).

NHC ring C1-N2-C3-C4-N5 of **5** adopts the perpendicular least hindered position with respect to the coordination plane Rh1-C1-C36-N30-N33 (89.9°) whereas the NHC ring C1-N2-C3-C4-N5 of **4** significantly deviates from the perpendicular arrangement (64.4°). In this regard, a thorough inspection of the structure of **4** revealed that a CH···π interaction involves the C41-H41 bond and the C18-C19-C20-C21-C22-C23 aromatic ring, reasonably forcing the NHC out of the perpendicular arrangement with respect to the coordination plane (Figure 3). In this connection, it is worth noting that the hydrogen-carbon distances H41-C18 (2.80 Å), H41-C19 (2.92 Å), H41-C20 (2.99 Å) H41-C21 (2.95 Å), H41-C22 (2.87 Å), H41-C23 (2.82 Å) are smaller than the sum of the Van der Waals radii of carbon and hydrogen (3.05 Å).

The NMR spectroscopic data confirm that the solid state structure of complexes is maintained in solution. Typical signals for pyridine, acetonitrile and IPr are observed in the ^{1}H NMR spectra of CD_2Cl_2 solutions of **4**–**6**, with no significant changes at low temperature, indicating fast rotation of the IPr ligand.[15b] Discrimination between the different disposition of the solvent molecules with regard to IPr can be achieved by ^{1}H-^{1}H-NOESY NMR experiments (Figure 4). Rather surprisingly, no exchange peaks were observed between both nitrogenated ligands in **4** or **5**, indicating a tight coordination. Besides, the ^{13}C{^{1}H}-APT NMR spectra are meaningful for detection of the carbon-coordinated ligands to rhodium. Thus, two doublets ascribed to IPr and CO were observed for **4** and **5** at $\delta > 170$ ppm, whereas the spectrum of the bis-carbonyl-IPr complex **6** displays three doublets in the same region. Moreover, ^{1}H-^{13}C HMBC correlation peaks between imidazolinyl protons and carbene-carbon atoms within IPr moieties facilitates the assignment of the Rh-C_{IPr} doublets. Resonances corresponding to carbonyl ligands ($\delta \approx 185$ ppm) are deshielded around 10 ppm with respect to those of IPr, which in turn appear slightly shielded with respect to the typical range observed for neutral Rh-IPr-CO[13c,7k,15b,16c,21] derivatives (δ 171–177 *vs* 182–186 ppm), likely as a consequence of a decrease of the electron density of the metallic center. The presence of two pyridine ligands in **4** was further confirmed by a ^{1}H-^{15}N HMQC NMR experiment. Two correlation peaks appear at δ 255.0 and 248.8 ppm, in the expected range for coordinated pyridines.[11c] The IR spectra of **4** and **5** show one strong CO stretching band at 1975 and 1988 cm^{-1}, respectively, whereas two bands at 2102 and 2031 cm^{-1} were observed for **6**, in agreement with a *cis* disposition of the CO ligands.

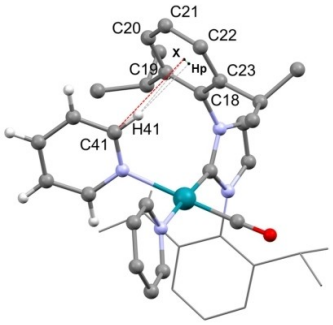

Figure 3. Brandl-Weiss view[20] of the C41-H41··· π interaction in **4**: C41-X 3.25 Å, C41-H41-X 132.6°, Hp–X 0.20 Å. Hp is the projection of H41 on the plane C18-C19-C20-C21-C22-C23, and X is the centroid of the C18-C19-C20-C21-C22-C23 ring.

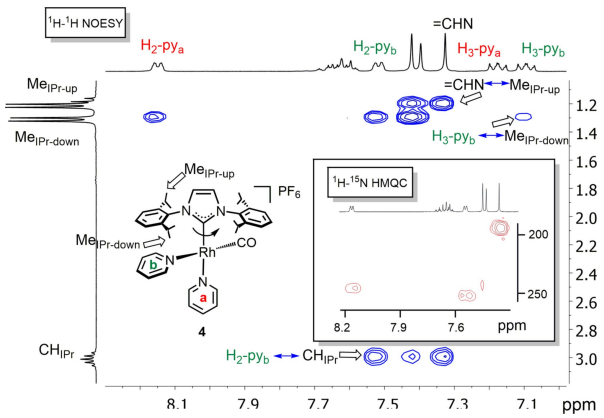

Figure 4. Selected regions of the ^{1}H-^{1}H NOESY, and ^{1}H-^{15}N HMQC NMR spectra of **4** in CD_2Cl_2.

An alternative access to cationic derivatives entails the extraction of chlorido ligand of the cod-derivative **1**. The acetonitrile-solvento complex [Rh(η^4-cod)(IPr)($NCCH_3$)][PF_6] (**7**) was cleanly prepared by treatment of **1** with $AgPF_6$ and isolated as a yellow microcrystalline solid in 72% yield (Scheme 2). Bubbling CO through a CH_2Cl_2 solution of **7** did not result in the expected substitution of the cod ligand, but instead the diolefin-CO complex [Rh(CO)(η^4-cod)(IPr)][PF_6] (**8**) was obtained. This unusual behavior is unprecedented for rhodium(I) chemistry,[22,23] although some examples has been reported for iridium.[24] As a curiosity, **8** is a nice example of *all metal-carbon bonds* complex.

The crystal structure of **7** and **8** shows a distorted square planar environment at the metal centre presenting a *cis* disposition of the NHC and the CH_3CN and CO ligands, respectively, with the [Rh(η^4-cod)(IPr)] moieties of **7** and **8** being virtually superimposable (Figure 5). Remarkably in both compounds the NHC C1-N2-C3-C4-N5 ring deviates from the perpendicular arrangement with respect to the related coordination plane Rh1-C1-CT01-CT02-N38 or Rh1-C1-CT01-CT02-C38 (**7**, 50.4°; **8**, 50.3°), which may be the consequence of the short contacts observed within the olefinic moiety C34-H34 and one aromatic wingtip of the NHC ligand (**7**, H34···C18 2.53 Å, H34···C23 2.63 Å; **8**, H34···C6, 2.62 Å; H34···C11, 2.61 Å). In agreement with the stronger *trans* influence of carbon monoxide *vs* acetonitrile the C34-C35 bond length in **7** [1.398(2) Å] is longer than in **8** [1.367(4) Å] whereas the rhodium-centroid distance is

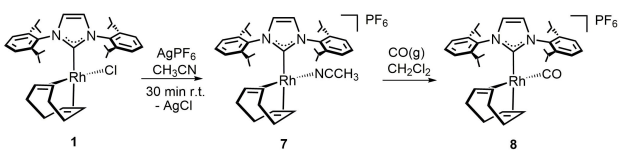

Scheme 2. Preparation of cationic complexes **7** and **8**.

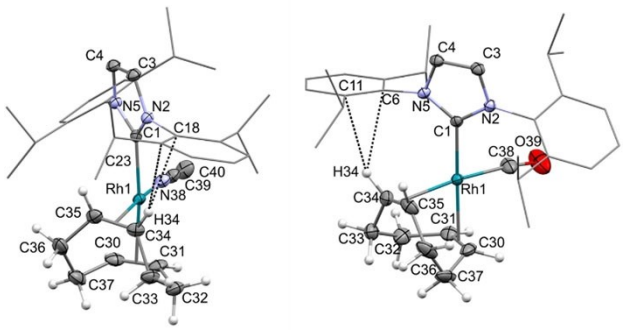

Figure 5. ORTEP view of [Rh(η^4-cod)(IPr)(CH_3CN)]$^+$ in **7** (*left*) and [Rh(η^4-cod)(IPr)(CO)]$^+$ in **8** (*right*) with ellipsoids at 50% probability. For clarity most hydrogen atoms are omitted and a wireframe style is adopted for the 2,5-$(iPr)_2C_6H_3$ moiety of the IPr ligand. Selected bond lengths (Å) and angles (°) are: **7**, C1-Rh1 2.0682(14), N38-Rh1 2.0536(14), Rh1-CT01 2.09156(14), C30-C31 1.380(3), Rh1-CT02 2.02291(13), C34-C35 1.398(2), N38-Rh1-C1 92.91(6), CT02-Rh1-CT01 86.628(6); **8**, Rh1-C1 2.067(2), Rh1-C38 1.870(3), C38-O39 1.137(3), Rh1-CT01 2.11478(19), C30-C31 1.380(4), Rh1-CT02 2.1710(2), C34-C35 1.367(4), C38-Rh1-C1 92.73(10), CT01-Rh1-CT02 84.271(8). CT01 and CT02 are the centroid of C30 and C31, and of C34 and C35, respectively.

shorter in **7** [2.02291(13) Å] than in **8** [2.1710(2) Å]. On the other hand, the C30-C31 bond lengths as well as the Rh-CT01 distances in **7** and **8** are virtually identical (**7**: C30-C31, 1.380(3) Å, Rh-CT01 2.09156(14) Å; **8**: C30-C31, 1.380(4) Å, Rh-CT01 2.11478(19) Å].

The NMR spectra of **7** and **8** display the typical signals for IPr and cod. Particularly, a singlet at δ 2.28 ppm, corresponding to the acetonitrile ligand, appears in the ^{1}H NMR spectrum of **7**, whereas a doublet at δ 180.4 ppm ($J_{C\text{-}Rh}$ = 77.2 Hz), ascribed to the CO ligand, is observed in $^{13}C\{^1H\}$-APT NMR spectrum of **8**. According to the solid structure, the very different *trans*-influence of acetonitrile and CO ligands is reflected in the chemical shift of the =CH resonances of the coordinated olefin (Figure 6). The $^{13}C\{^1H\}$-APT NMR spectrum of the acetonitrile derivative **7** displays a doublet at δ 78.2 ppm, which is downfield shifted around 36 ppm for the CO counterpart **8**. Moreover, the $J_{C\text{-}Rh}$ decreases from 13.2 to 5.6 Hz as a consequence of longer separation between rhodium and η^2-olefin. In addition, a strong CO stretching band at 2037 cm^{-1} was observed in the IR spectra of **8**.

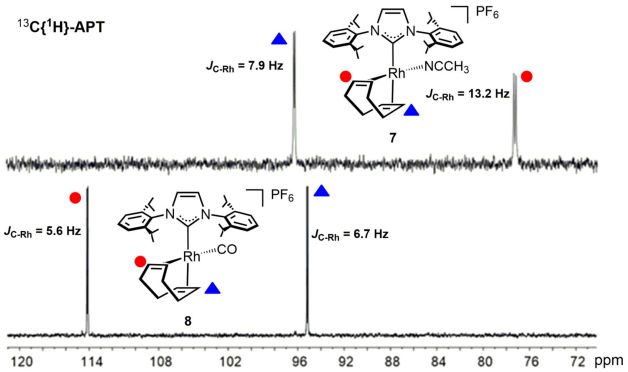

Figure 6. Selected region of the $^{13}C\{^1H\}$-APT NMR spectra showing the Rh-cod resonances for **7** and **8**.

Synthesis of neutral Rh-IPr complexes with π-acceptor ligands

We sought to study the influence of the coordination of π-acceptor ligands different to CO, namely isocyanides and phosphites, on the structure and properties of Rh-IPr complexes. Isocyanides (R–N≡C) have an isoelectronic structure with carbon monoxide, being better σ-donors and poorer π-acceptors.[8] In other way, the π-acceptor character of phosphites relies on their alkoxy substituents. The introduction of this conically structured ligand allows to create a more complex sterical interplay between NHC and the π-acid moiety, rather limited with linear ligands such as CO.[9] Thus, treatment of **3** with 2 equivalents of tert-butyl isocyanide (^{t}BuNC) or trimethyl phosphite gives the bis-substituted neutral complexes [RhCl($CN^tBu)_2$(IPr)] (**9**, 61% yield) or [RhCl(IPr){$P(OMe)_3$}$_2$] (**10**, 68% yield), respectively (Scheme 3). It is noteworthy that Rh–NHC complexes bearing isocianyde[25] or phosphite[26] ligands are scarce.

The crystal structure of **9** and **10** reveals a distorted square planar geometry for the metal centre with a *cis* disposition of the NHC and the chlorido ligands [**9**, C1-Rh–Cl 85.47(5)°; **10**, C1-Rh1-Cl1 91.54(6)°] (Figure 7). The two remaining coordination sites are occupied by tert-butyl isocyanido [**9**, C36-Rh–C30 86.65(7)°] or trimethyl phosphite [**10**, P2-Rh1-P1 90.58(2)°]. As a consequence of the higher *trans* influence of the NHC ligand when compared with the chlorido ligand, the Rh–C30 and Rh–C36 bond lengths in **9** as well as the Rh–P1 and Rh–P2 bond lengths in **10** are different. Indeed, Rh–P1 and Rh–C30 (*trans* to C1) are longer than Rh–P2 and Rh–C36 (*trans* to chlorido), respectively. It is worth mentioning that both in **9** and in **10** the NHC ring slightly deviates from the perpendicular arrangement with respect to coordination plane (**9**, 79.3°; **10**, 73.6°). A thorough examination of the structure did not reveal any intramolecular contacts that could be responsible for this deviation, so it can be argued that it is reasonably the consequence of the crystal packing, or possibly of subtle electronic effects. Finally, the bond angles within the tert-butyl isocyanido ligand *cis* to the NHC moiety are remarkable. As a matter of fact, the Rh–C36-N37 [172.40(16)°] and the C36-N37-C38 [156.13(18)°] angles deviate from the ideal value of 180° probably as a consequence of the steric repulsion between the NHC wingtips and the tert-butyl group.

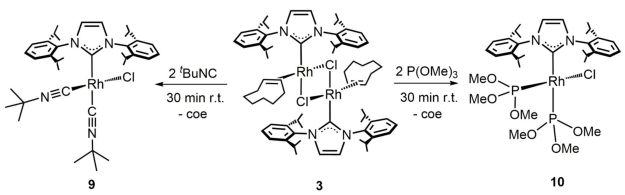

Scheme 3. Preparation of neutral complexes **9** and **10**.

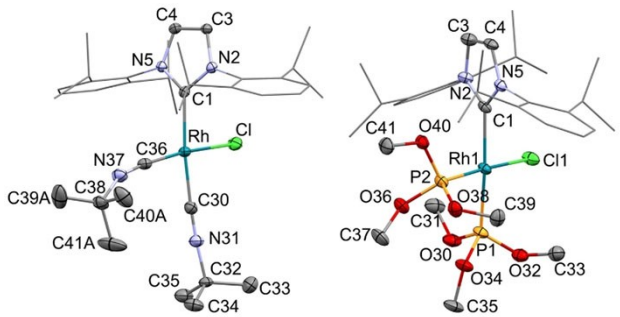

Figure 7. ORTEP view of [RhCl(CN^{t}Bu)$_2$(IPr)] (**9**) (*left*) and [RhCl(IPr){P(OMe)$_3$}$_2$] (**10**) (*right*) with ellipsoids at 50% probability. For clarity hydrogen atoms are omitted and a wireframe style is adopted for the 2,5-(iPr)$_2$C$_6$H$_3$ moiety of the IPr ligand. Selected bond lengths (Å) and angles (°) are: **9**, C1-Rh 2.0512(16), C30-Rh 1.9389(18), C30-N31 1.158(2), C36-N37 1.173(2), C36-Rh 1.8674(18), C1-Rh–Cl 85.47(5), C36-Rh–C30 86.65(7), C30-Rh–C1 172.74(7), C36-Rh–C1 100.54(7), C30-N31-C32 175.62(19), C36-N37-C38 156.13(18), N37-C36-Rh 172.40(16), N31-C30-Rh 176.85(17); **10**, C1-Rh1 2.070(2), P1-Rh1 2.2131(6), P2-Rh1 2.1461(7), C1-Rh1-P2 92.19(6), C1-Rh1-P1 172.63(6), P2-Rh1-P1 90.58(2), C1-Rh1-Cl1 91.54(6).

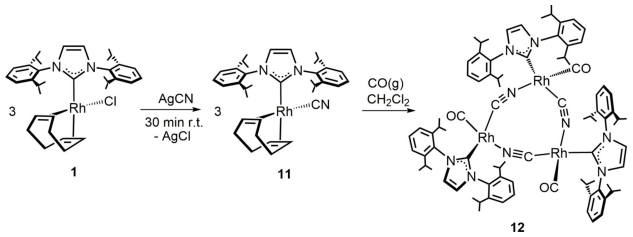

Scheme 4. Preparation of neutral complexes **11** and **12**.

The more noticeable feature of the NMR data of **9** was the appearance of three doublets in the $^{13}C\{^1H\}$-APT spectrum at δ 193.6 ($J_{C\text{-}Rh}$ = 45.0 Hz), 161.2 ($J_{C\text{-}Rh}$ = 71.8 Hz), and 150.4 ppm ($J_{C\text{-}Rh}$ = 52.6 Hz), which are ascribed to IPr and each isocyanido ligands, respectively. Regarding to **10**, the signal of the carbene carbon atom is observed at δ 192.1 ppm as a doublet of doublets of doublets in the $^{13}C\{^1H\}$-APT spectrum, as a result of C–Rh (45.7 Hz) and C–P (167.4 and 12.6 Hz) couplings. In agreement with the proposed structure, the $^{31}P\{^1H\}$ spectrum of **10** displays two doublets of doublets at δ 143.7 and 141.6 ppm with $J_{P\text{-}P}$ = 63.0 Hz and $J_{P\text{-}Rh}$ = 159.9 and 263.3 Hz, respectively. It is interesting to note, that the carbene resonance of **9** and **10** is downfield shifted by around 15–20 ppm related to Rh–CO derivatives, indicating that CO is a much stronger π-acceptor than isocyanido or phosphito ligands.

A second synthetic strategy to introduce a π-acid moiety in the Rh–NHC framework is the replacement of the chlorido ligand in **1** by an anionic π-acceptor ligand, such as cyanide. The cyanide anion is isoelectronic and isosteric with CO, however, the small variance in electronegativity between C and N atoms makes the energy on the lone pair at the C atom similar to that of N. For this reason, and in contrast to the CO ligand, N≡C$^-$ can act as a 1κ*C*,2κ*N* bridging ligand between two metals.[27] In addition, the negative charge makes N≡C$^-$ a stronger σ-donor. The total charge is also responsible for the higher π*-orbitals energy compared to CO, making cyanide a weaker π-acceptor than CO. NHC-cyanido transition metal complexes have recently received an increasing attention for their interesting photochemical properties.[28] Thus, treatment of complex **1** with AgCN gave the neutral complex Rh(CN)(η^4-cod)(IPr) (**11**) which was isolated as a yellow solid in 73% yield (Scheme 4). Similarly to **8**, compound **11** has exclusively carbon donor ligands. Decoordination of chelate cod could be carried out by bubbling CO(g) through a CH_2Cl_2 solution of **11** resulting in the formation of the cyano-bridged trinuclear complex [Rh{1κ*C*,2κ*N*-(CN)}(CO)(IPr)]$_3$ (**12**) (see below).

The structure of the cyanido complexes **11** and **12** was elucidated by X-ray structural analysis (Figure 8). The coordination environment of rhodium in the crystal structure of **11** is distorted square planar, the NHC and cyanide ligands occupying two *cis* positions [C38-Rh–C1 88.56(8)°]. The olefinic carbon-carbon bond lengths [C30-C31 1.376(3) Å, C34-C35 1.391(3) Å] as well as the rhodium-centroids distances are similar [Rh-CT01 2.0925(4) Å, Rh-CT02 2.0657(4) Å], suggesting that the *trans* influence of the NHC and cyanide ligands in **11** is similar. Finally, when compared with the cod derivatives **7** and **8**, the NHC core C1-N2-C3-C4-N5 deviates from the perpendicular arrangement with respect to the coordination plane Rh–C1-CT01-CT02-C38 to a lesser extent (71.6°) and the examination of the crystal structure did not reveal any intermolecular contacts.

The crystal structure of **12** reveals a trinuclear motif supported by bridging 1κ*C*,2κ*N*-cyanido ligands in which the [Rh(CN)]$_3$ core slightly deviates from planarity (max deviation 0.23 Å; mean absolute deviation 0.13 Å). The square planar environment at each rhodium centre is completed by one NHC and one carbon monoxide ligand (C^{CO}-Rh-C^{NHC}, 95.0°, av.). The three [Rh(IPr)(CO)(κ*C*–CN)(κ*N*-NC)] fragments are crystallographically independent, nonetheless similar bond lengths and angles are observed. Remarkably, the Rh-C–N-Rh fragments deviate from linearity reasonably in order for the square planar metal moieties to fit in the trinuclear core [Rh-C^{CN}-N^{CN}, 169.2°, av.; Rh-N^{CN}-C^{CN}, 161.6°, av.]. Accordingly, the angles C^{CN}-Rh-N^{CN} (84.4°, av.) deviate from the expected value for a square planar geometry.

The formation of a multinuclear architecture supported by cyanido-bridged ligands is remarkable but not unprecedented.[27] Heteronuclear tetrameric pseudoplanar structures involving Rh–Co,[27b] Rh–Ru[27c] or Co–Ni[27d] pairs or even cubane-type clusters[27b–c] have been described previously. Particularly, Hawthorne *et al.* described a rhodium trinuclear complex related to **12** bearing phosphines and carboranes as ancillary ligands.[27a] The NMR spectra of **12** show that the cyanido-bridged structure is maintained in solution. Thus, while the carbon atom of the cyanide ligand in **11** appears as a doublet at δ 141.0 ppm ($J_{C\text{-}Rh}$ = 45.0 Hz) in the $^{13}C\{^1H\}$-APT spectrum, the equivalent cyanide ligands of **12** are observed as a doublet of doublets at 156.5 ppm as a result of a direct $^1J_{C\text{-}Rh}$ of 45.4 Hz and a $^2J_{C\text{-}Rh}$ of 5.4 Hz arising within the Rh–C≡N–Rh moiety (Figure 9). Although the actual nuclearity of **12** in

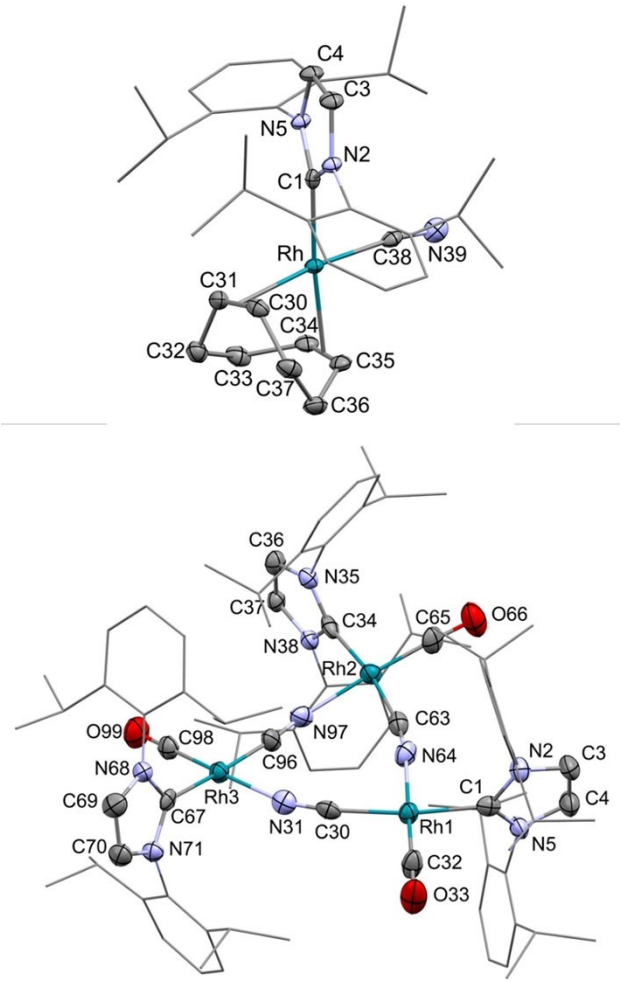

Figure 8. ORTEP view of [Rh(CN)(η^4-cod)(IPr)] (**11**) (*top*) and [Rh(1κ*C*,2κ*N*-CN)(CO)(IPr)]$_3$ (**12**) (*bottom*) with ellipsoids at 50% probability. For clarity hydrogen atoms are omitted and a wireframe style is adopted for the 2,5-(iPr)$_2$C$_6$H$_3$ moiety of the IPr ligand. Selected bond lengths (Å) and angles (°) are: **11**, C1-Rh 2.060(2), C38-Rh 2.034(2), C38-N39 1.123(3), Rh-CT01 2.0925(4), C30-C31 1.376(3), Rh-CT02 2.0657(4), C34-C35 1.391(3), C38-Rh–C1 88.56(8), CT02-Rh-CT01 85.83(2), CT01 and CT02 are the centroid of C30 and C31, and of C34 and C35, respectively; **12**, C1-Rh1 2.029(7), C32-Rh1 1.785(8), C30-Rh1 2.014(8), C30-N31 1.160(8), N64-Rh1 2.036(6), C34-Rh2 2.020(7), C65-Rh2 1.778(8), C63-Rh2 1.990(8), C63-N64 1.158(8), N97-Rh2 2.073(6), C67-Rh3 2.024(7), C98-Rh3 1.768(7), C96-Rh3 1.981(8), C96-N97 1.157(8), N31-Rh3 2.079(6), C32-Rh1-C1 95.0(3), C30-Rh1-C1 168.9(3), C30-Rh1-N64 84.9(2), C65-Rh2-C34 95.6(3), C34-Rh2-N97 89.2(2), C63-Rh2-N97 81.2(2), C98-Rh3-C67 94.2(3), C96-Rh3-C67 174.9(3), C67-Rh3-N31 91.5(2), C96-Rh3-N31 87.1(2), N31-C30-Rh1 166.6(6), C30-N31-Rh3 158.0(6).

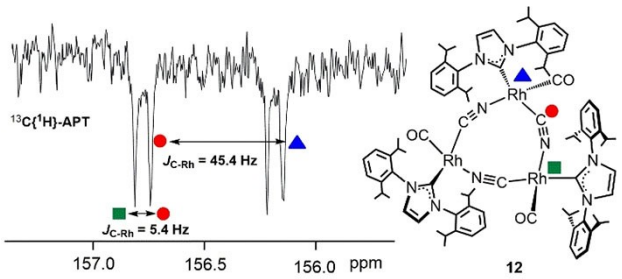

Figure 9. Selected region of the ^{13}C{^{1}H}-APT NMR spectra of **12** showing the Rh–C≡N–Rh resonance.

solution cannot be undoubtedly determined, we assume the trinuclear structure to be the most likely, in accordance to that observed in the solid state. In addition, a strong CO stretching band at 1954 cm^{-1} was observed in the IR spectra of **12**.

Catalytic activity for phenylacetylene-methanol transformations

Hydroalkoxylation of alkynes is a straightforward method for the preparation of enol ethers. The groups of Messerle[7f] and Bera[7h] have shown that Rh–NHC complexes bearing CO ligands are efficient catalysts for these transformations. Thus, we have studied the catalytic activity of complexes **1**–**12** for the addition of methanol to phenylacetylene. After a preliminary screening of different solvents and temperatures, a mixture of MeOH/DMA (1:1, 2 mL) (DMA = dimethylacetamide) using 1 mmol of alkyne and 2 mol% catalyst loading at 70 °C for 24 h were established as optimal conditions[7h] (Scheme 5, Table 1). The catalytic outcome is strongly dependent on the catalyst. In addition to the expected alkyne hydroalkoxylation to enol ethers (**16**), alkyne polymerization (**13**),[29] cyclotrimerization (**14**)[30] or dimerization (**15**)[12c] were also observed. The new dienol ethers (**17**)[31] resulting from formal addition of methanol to enynes **15** were also formed in some cases. The best catalyst for hydroalkoxylation of phenylacetylene to form **16** was the previously prepared neutral dicarbonyl complex **2**. A conversion of 75% with 58:39 *E:Z* selectivity was obtained (entry 2). Among the new catalysts, only the isocyanido complex **9** promotes the formation of enol ethers with 17:50 *E:Z* selectivity, although 31% of enynes **15** arisen from dimerization were also observed (entry 9). Participation of methanol as substrate took place also for the cationic carbonyl derivatives **5**, **6**, and **8**, but to yield the dienol ethers **17** (entries 5, 6, and 8). The remaining catalysts promoted the transformation of phenylacetylene without involvement of methanol. Thus, the cod complexes **1**, **7**, and **11**, lacking the CO moiety, polymerized phenylacetylene, although with formation of variable amounts of cyclotrimerization or dimerization products (entries 1, 7 and 11). The bis-pyridine complex **4** is inefficient as catalyst only converting 15% of phenylacetylene to unidentified products (entry 4). The presence of methanol did not significantly affect the catalytic performance of coe dimer **3**, which has been previously found to promote the cyclotrimerization and dimerization of phenylacetylene (entry 3).[11c] The phosphite complex

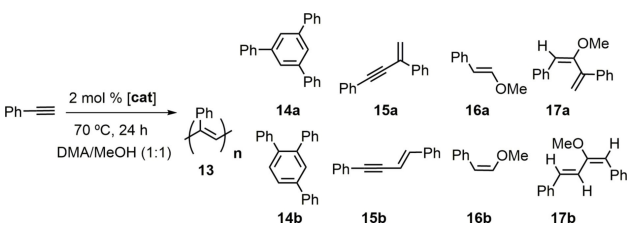

Scheme 5. Reaction products in the catalytic transformation of phenylacetylene in MeOH/DMA.

Table 1. Phenylacetylene transformations in MeOH/DMA with catalysts **1**–**12**.[a]

Entry	Cat.	Conv. (%)	Polymer	Trimer **14a/b**	Dimer **15a/b**	Enol ether **16a/b**	Dienol ether **17a/b**[b]
1	**1**	81	38	42/20	–	–	–
2	**2**	75	–	–	–	60/38	2
3	**3**	24	–	15/55	28/2	–	–
4	**4**	15	–	–	–	–	–
5	**5**	55	–	–	–	–	39/61
6	**6**	52	–	–	–	–	40/60
7	**7**	>99	34	8/9	36/13	–	–
8	**8**	87	–	–	–	–	39/61
9	**9**	74	–	–	13/18	17/50	2
10	**10**	>99	–	–	98/2	–	–
11	**11**	>99	87	2/3	4/4	–	–
12	**12**	>99	–	–	74/26	–	–

[a] Reaction conditions: 1 mmol of phenylacetylene, 1 mL of methanol, 0.02 mmol of catalyst, 1 mL of DMA (dimethylacetamide), 70 °C, 24 h. [b] Determinated by GC as isomers mixture.

10 is the most efficient among the catalysts presented in this study. Almost full conversion of phenylacetylene was attained with 98% selectivity to the *gem*-enyne **15a** (entry 10), although it is not competitive with other Rh–NHC alkyne dimerization catalysts.[11h,12c] Finally, the cyanido trimer **12** also promotes alkyne dimerization but less selectively (entry 12).

The results presented in Table 1 show divergent catalytic outcomes depending on the π-acceptor ligand and the charge of the catalyst. It has been previously proposed that hydroalkoxylation of alkynes promoted by rhodium catalysts proceeds via vinylidene and alkoxycarbene intermediates, which were stabilized by a π-acceptor ligand (Scheme 6).[7h,32] In accordance to that, the neutral Rh-IPr-CO complex **2** is the most efficient catalyst for the formation of enol ethers. The introduction of a less π-acidic ligand such as isocyanido in **9**, resulted in a slightly lower selectivity and the concomitant formation of enyne dimers. In fact, catalysts bearing ligands of lower π-acceptor ability such as phosphito (**10**) and cyanido (**12**) selectively afforded dimerization products. Regarding catalyst charge, cationic Rh–CO complexes **5**, **6**, and **8** promote the formation of dienol ethers. A rational explanation could arise from the presence of an extra vacant site with regard to neutral counterparts which allows the coordination of a second molecule of alkyne to yield a [2+2] coupling with the alkoxycarbene intermediate resulting in the formation of dienol ethers.[33] As previously described,[29] Rh-cod complexes **1**, **7**, and **11**, lacking a π-acceptor ligand, promoted the polymerization of phenylacetylene.

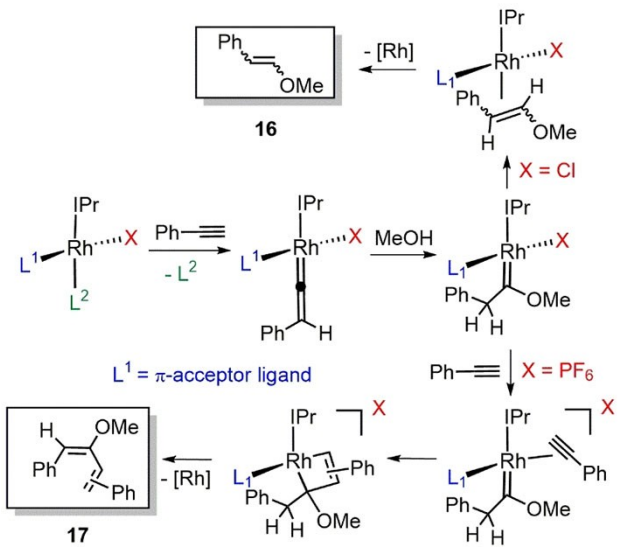

Scheme 6. Tentative mechanistic proposal for the hydroalkoxylation reactions.

Conclusion

A series of neutral and cationic Rh-IPr complexes bearing different π-acceptor ligands have been prepared. Chlorido abstraction in [RhCl(η^4-cod)(IPr)] afforded the cationic solvento complex [Rh(η^4-cod)(IPr)(NCCH$_3$)]$^+$, whereas the cationic bis-solvento derivatives [Rh(CO)(IPr)(L)$_2$]$^+$ (L = py, CH$_3$CN) were obtained from RhCl(CO)$_2$(IPr) by replacement of the *trans*-IPr CO ligand by pyridine or acetonitrile. The bis-acetonitrile derivative reversibly reacted with CO to afford the bis-carbonyl compound Rh(CO)$_2$(IPr)(NCCH$_3$)]$^+$. In sharp contrast, the carbonylation of [Rh(η^4-cod)(IPr)(NCCH$_3$)]$^+$ did not result in the decoordination of the diolefin but the unexpected cod-carbonyl compound [Rh(η^4-cod)(IPr)(CO)]$^+$ was obtained. Alternatively, neutral derivatives of formulation RhCl(IPr)(L)$_2$ {L = ^{t}BuNC or P(OMe)$_3$} were prepared from [Rh(μ-Cl)(η^2-coe)(IPr)]$_2$ by reaction with ^{t}BuNC or P(OMe)$_3$. Anion exchange of the chlorido ligand in RhCl(η^4-cod)(IPr) by cyanide afforded the mononuclear complex Rh(CN)(η^4-cod)(IPr). However, carbonylation of this compound resulted in the displacement of the cod ligand and the formation of the unusual trinuclear carbonyl compound [Rh{1κ*C*,2κ*N*-(CN)}(CO)(IPr)]$_3$ supported by bridging cyanido ligands.

The catalytic performance of the new Rh-IPr complexes for the addition of methanol to phenylacetylene has been studied. It has been found that the catalytic outcome is strongly dependent on the Rh-IPr-π-acceptor catalyst. Thus, the neutral bis-CO or bis-isocyanido catalysts promote the hydroalkoxyla-

tion reaction to yield enol ethers, whereas the bis-phosphito and bis-cyanido precursors favors alkyne dimerization. In contrast, cationic CO-derivatives afford dienol ether derivatives resulting from the triple coupling of two alkynes and methanol. Finally, Rh-cod complexes promote the polymerization of phenylacetylene. The results reported herein highlight how a slight fine-tuninig of the stereoelectronic properties of the catalyst results in divergent catalytic outcomes.

Experimental Section

General Considerations. All reactions were carried out with rigorous exclusion of air and moisture using Schlenk-tube techniques and dry box when necessary. The organometallic precursors RhCl(η^4-cod)(IPr)[13a] (**1**), RhCl(CO)$_2$(IPr)[13c] (**2**), and [Rh(μ-Cl)(IPr)(η^2-coe)]$_2$[13b] (**3**), were prepared as previously described in the literature. Chemical shifts (expressed in parts per million) are referenced to residual solvent peaks (^{1}H and ^{13}C{^{1}H}), NH_3 (^{15}N), H_3PO_4 (^{31}P), or $CFCl_3$ (^{19}F). Coupling constants, *J*, are given in Hz. Spectral assignments were achieved by combination of ^{1}H-^{1}H COSY, ^{13}C{^{1}H}-APT and ^{1}H-^{13}C HSQC/HMBC experiments.

Preparation of [Rh(CO)(IPr)(py)$_2$][PF$_6$] (4): A yellow solution of **2** (200 mg, 0.345 mmol) in 10 mL of pyridine protected from light by an aluminium foil was treated with thallium(I) hexafluorophosphate (130 mg, 0.372 mmol) and it was stirred at room temperature for 30 min. Then, the suspension was filtered through celite and the solvent was evaporated to dryness. The resulting solid was dissolved in 10 mL of dichloromethane, filtered again and concentrated to ca. 1 mL. Addition of diethyl ether induced the precipitation of a light yellow solid, which was washed with diethyl ether (3×5 mL) and dried in vacuo. Yield: 187 mg (65%). Anal. Calcd. for $C_{38}H_{46}N_4F_6OPRh$: C, 55.48; H, 5.64; N, 6.81. Found: C, 55.27; H, 5.44; N, 7.01. IR (cm^{-1}, ATR): 1975 ν(CO). HRMS (ESI$^+$) *m/z* Calc for $RhC_{33}H_{41}N_3O$ (M$^+$-py): 598.2299 Exp: 598.2298. ^{1}H NMR (400.2 MHz, CD_2Cl_2, 298 K): δ 8.12 (m, 2H, $H_{2\text{-}py\text{-}a}$), 7.59 (m, 4H, $H_{p\text{-}Ph}$, $H_{4\text{-}py\text{-}b}$, $H_{4\text{-}py\text{-}a}$), 7.48 (m, 2H, $H_{2\text{-}py\text{-}b}$), 7.38 (d, $J_{H\text{-}H}$ = 7.8, 4H, $H_{m\text{-}Ph}$), 7.29 (s, 2H, =CHN), 7.14 (m, 2H, $H_{3\text{-}py\text{-}a}$), 7.06 (m, 2H, $H_{3\text{-}py\text{-}b}$), 2.98 (sept, $J_{H\text{-}H}$ = 6.8, 4H, C$\underline{H}$Me$_{IPr}$), 1.28 (d, $J_{H\text{-}H}$ = 6.8, 12H, Me$_{IPr\text{-}down}$), 1.18 (d, $J_{H\text{-}H}$ = 6.8, 12H, Me$_{IPr\text{-}up}$). ^{13}C{^{1}H}-APT NMR (100 MHz, CD_2Cl_2, 298 K) δ 189.5 (d, $J_{C\text{-}Rh}$ = 78.7, CO), 176.9 (d, $J_{C\text{-}Rh}$ = 56.0, Rh-C$_{IPr}$), 151.0 (s, $C_{2\text{-}py\text{-}a}$), 150.3 (s, $C_{2\text{-}py\text{-}b}$), 146.5 (s, $C_{q\text{-}IPr}$), 139.6, (s, $C_{3\text{-}py\text{-}b}$), 139.1, (s, $C_{3\text{-}py\text{-}a}$), 136.2 (s, C_qN), 131.1, (s, $CH_{p\text{-}Ph}$), 126.4 (s, $C_{4\text{-}py\text{-}b}$), 126.3 (s, $C_{4\text{-}py\text{-}a}$), 125.7 (s, =CHN), 125.2 (s, $CH_{m\text{-}Ph}$), 29.6 (s, C$\underline{H}$Me$_{IPr}$), 26.3 (s, Me$_{IPr\text{-}up}$), 22.9 (s, Me$_{IPr\text{-}down}$). ^{19}F NMR (282 MHz, CD_2Cl_2, 298 K): δ −73.1 (d, $J_{F\text{-}P}$ = 713.5, PF_6). ^{31}P NMR (121 MHz, CD_2Cl_2, 298 K): δ −144.6 (sept, $J_{P\text{-}F}$ = 713.5, PF_6). ^{1}H-^{15}N HMQC NMR (40.5 MHz, CD_2Cl_2, 298 K): δ 255.0 ($N_{py\text{-}b}$), 248.8 ($N_{py\text{-}a}$),194.5 (N_{IPr}).

Preparation of [Rh(CO)(IPr)(NCCH$_3$)$_2$][PF$_6$] (5): This complex was prepared as described for **1**, starting from **2** (700 mg, 1.208 mmol) and thallium(I) hexafluorophosphate (464 mg, 1.328 mmol) in 20 mL of acetonitrile. Yield: 736 mg (82%). Anal. Calcd. for (M+H_2O), $C_{32}H_{42}F_6N_4OPRh.H_2O$: C, 50.27; H, 5.80; N, 7.33. Found: C, 50.40; H, 5.86; N, 6.98. IR (cm^{-1}, ATR): 1988 ν(CO). HRMS (ESI$^+$): *m/z* Calc for $RhC_{30}H_{39}N_3O$: (M$^+$-CH_3CN): 560.2143 Exp: 560.2201. ^{1}H NMR (400 MHz, CD_2Cl_2, 213 K): δ 7.64 (t, $J_{H\text{-}H}$ = 7.8, 2H, $H_{p\text{-}Ph}$), 7.44 (d, $J_{H\text{-}H}$ = 7.8, 4H, $H_{m\text{-}Ph}$), 7.32 (s, 2H, =CHN), 2.51 (sept, $J_{H\text{-}H}$ = 6.7, 4H, C$\underline{H}$Me$_{IPr}$), 2.31 (s, 3H, NCC$H_{3\text{-}cis\text{-}IPr}$), 2.16 (s, 3H, NCC$H_{3\text{-}trans\text{-}IPr}$), 1.34 (d, $J_{H\text{-}H}$ = 6.7, 12H, Me$_{IPr\text{-}down}$), 1.15 (d, $J_{H\text{-}H}$ = 6.7, 12H, Me$_{IPr\text{-}up}$). ^{13}C{^{1}H}-APT NMR (100 MHz, CD_2Cl_2, 213 K): δ 185.0 (d, $J_{C\text{-}Rh}$ = 80.0, CO), 171.8 (d, $J_{C\text{-}Rh}$ = 52.3, Rh-C$_{IPr}$), 145.8 (s, $C_{q\text{-}IPr}$), 134.7 (s, C_qN), 130.9 (s, $CH_{p\text{-}Ph}$), 126.0 (s, =CHN), 124.5 (s, $CH_{m\text{-}Ph}$), 122.6 (d, $J_{C\text{-}Rh}$ = 7.6, N$\underline{C}$CH$_{3\text{-}cis\text{-}IPr}$), 121.6 (d, $J_{C\text{-}Rh}$ = 7.1, N$\underline{C}$CH$_{3\text{-}trans\text{-}IPr}$), 28.9 (s, C$\underline{H}Me_{IPr}$), 26.2 (s, Me$_{IPr\text{-}up}$), 22.3 (s, Me$_{IPr\text{-}down}$), 3.9 (s, NC$\underline{C}H_{3\text{-}cis\text{-}IPr}$), 3.8 (s, NC$\underline{C}H_{3\text{-}trans\text{-}IPr}$). ^{19}F NMR (282 MHz, CD_2Cl_2, 298 K): δ −73.1 (d, $J_{F\text{-}P}$ = 713.5, PF_6). ^{31}P NMR (121 MHz, CD_2Cl_2, 298 K): δ −144.6 (sept, $J_{P\text{-}F}$ = 713.5, PF_6).

Preparation of [Rh(CO)$_2$(IPr)(NCCH$_3$)][PF$_6$] (6): Carbon monoxide was bubbled through a yellow solution of **5** (100 mg, 0.134 mmol) in 20 mL of dichloromethane at room temperature for 10 min. The solution was concentrated to ca. 1 mL and diethyl ether was added to induce the precipitation of a light yellow solid, which was washed with diethyl ether (3×5 mL) and dried in vacuo. Yield: 74 mg (71%). Anal. Calcd. for $C_{31}H_{39}F_6N_3O_2PRh$: C, 50.76; H, 5.36; N, 5.73. Found: C, 50.72; H, 5.39; N, 5.82. IR (cm^{-1}, ATR): 2102, ν_a(CO), 2031 ν_s(CO). HRMS (ESI$^+$) *m/z* Calc for $RhC_{30}H_{39}N_3O$: (M$^+$-CO): 560.2143 Exp: 560.2156. ^{1}H NMR (400 MHz, CD_2Cl_2, 233 K): δ 7.62 (t, $J_{H\text{-}H}$ = 7.8, 2H, $H_{p\text{-}Ph}$), 7.43 (d, $J_{H\text{-}H}$ = 7.8, 4H, $H_{m\text{-}Ph}$), 7.41 (s, 2H, =CHN), 2.53 (sept, $J_{H\text{-}H}$ = 6.8, 4H, C$\underline{H}$Me$_{IPr}$), 2.36 (s, 3H, NCCH_3), 1.35 and 1.16 (both d, $J_{H\text{-}H}$ = 6.8, 24H, Me$_{IPr}$). ^{13}C{^{1}H}-APT NMR (100 MHz, CD_2Cl_2, 233 K): δ 182.2 (d, $J_{C\text{-}Rh}$ = 75.6, $CO_{cis\text{-}IPr}$), 181.1 (d, $J_{C\text{-}Rh}$ = 53.3, $CO_{trans\text{-}IPr}$), 171.0 (d, $J_{C\text{-}Rh}$ = 44.6, Rh-C$_{IPr}$), 145.4 (s, $C_{q\text{-}IPr}$), 133.7 (s, C_qN), 131.3 (s, $CH_{m\text{-}Ph}$), 126.6 (s, =CHN), 126.1 (br, N$\underline{C}$CH$_3$), 124.7 (s, $CH_{p\text{-}Ph}$), 29.0 (s, C$\underline{H}$Me$_{IPr}$), 26.2 and 22.4 (both s, Me$_{IPr}$), 4.3 (s, NC$\underline{C}$H$_3$). ^{19}F NMR (282 MHz, CD_2Cl_2, 298 K): δ −73.1 (d, $J_{F\text{-}P}$ = 713.5, PF_6). ^{31}P NMR (121 MHz, CD_2Cl_2, 298 K): δ −144.6 (sept, $J_{P\text{-}F}$ = 713.5, PF_6).

Preparation of [Rh(η^4-cod)(IPr)(NCCH$_3$)][PF$_6$] (7): The complex was prepared as described for **5**, starting from **1** (200 mg, 0.315 mmol) and silver(I) hexafluorophosphate (80 mg, 0.316 mmol). A microcrystalline yellow solid was obtained. Yield: 176 mg (72%). Anal. Calcd. for $C_{37}H_{51}F_6N_3PRh$: C, 56.56; H, 6.54; N, 5.35; Found: C, 56.24; H, 6.52; N, 5.52. HRMS (ESI$^+$) *m/z* Calc for $RhC_{35}H_{48}N_2$ (M$^+$-CH_3CN): 599.2867 Exp: 599.2894. ^{1}H NMR (300 MHz, CD_2Cl_2, 298 K): δ 7.65 (t, $J_{H\text{-}H}$ = 7.8, 2H, $H_{p\text{-}Ph}$), 7.47 (d, $J_{H\text{-}H}$ = 7.8, 4H, $H_{m\text{-}Ph}$), 7.25 (s, 2H, =CHN), 4.34 (m, 2H, =$CH_{cod\text{-}trans\text{-}IPr}$), 3.71 (m, 2H, =$CH_{cod\text{-}cis\text{-}IPr}$), 2.70 (sept, $J_{H\text{-}H}$ = 6.8, 4H, C$\underline{H}$Me$_{IPr}$), 2.28 (s, 3H, NCCH_3), 2.0–1.7 (8H, $CH_{2\text{-}cod}$), 1.45 and 1.20 (both d, $J_{H\text{-}H}$ = 6.8, 24H, Me$_{IPr}$). ^{13}C{1H}-APT NMR (75 MHz, CD_2Cl_2, 298 K): δ 178.9 (d, $J_{C\text{-}Rh}$ = 52.1, Rh-C$_{IPr}$), 145.7 (s, $C_{q\text{-}IPr}$), 135.0 (s, C_qN), 130.7 (s, $CH_{p\text{-}Ph}$), 125.8 (s, =CHN), 124.6 (br, N$\underline{C}$CH$_3$), 124.3 (s, $CH_{m\text{-}Ph}$), 96.2 (d, $J_{C\text{-}Rh}$ = 7.9, $CH_{cod\text{-}trans\text{-}IPr}$), 78.2 (d, $J_{C\text{-}Rh}$ = 13.2, $CH_{cod\text{-}cis\text{-}IPr}$), 31.7 and 28.4 (both s, $CH_{2\text{-}cod}$), 29.0 (s, C$\underline{H}$Me$_{IPr}$), 26.1 and 22.5 (both s, Me$_{IPr}$), 4.0 (s, NC$\underline{C}$H$_3$). ^{19}F NMR (282 MHz, CD_2Cl_2, 298 K): δ −73.1 (d, $J_{F\text{-}P}$ = 713.5, PF_6). ^{31}P NMR (121 MHz, CD_2Cl_2, 298 K): δ −144.6 (sept, $J_{P\text{-}F}$ = 713.5, PF_6).

Preparation of [Rh(CO)(η^4-cod)(IPr)][PF$_6$] (8): The complex was prepared as described for **6** starting from **7** (100 mg, 0.127 mmol) and obtained as a yellow solid. Yield: 57 mg (57%). Anal. Calcd. for $C_{36}H_{48}F_6N_2OPRh$: C, 55.96; H, 6.26; N, 3.63; Found: C, 55.85; H, 6.15; N, 3.49. IR (cm^{-1}, ATR): 2037 ν(CO). HRMS (ESI$^+$) *m/z* Calc for $RhC_{35}H_{48}N_2$: (M$^+$-CO): 599.2867 Exp: 599.2884. ^{1}H NMR (300 MHz, CD_2Cl_2, 298 K): δ 7.67 (t, $J_{H\text{-}H}$ = 7.8, 2H, $H_{p\text{-}Ph}$), 7.48 (s, 2H, =CHN), 7.46 (d, $J_{H\text{-}H}$ = 7.8, 4H, $H_{m\text{-}Ph}$), 5.16 (m, 2H, $CH_{cod\text{-}cis\text{-}IPr}$), 4.75 (m, 2H, $CH_{cod\text{-}trans\text{-}IPr}$), 2.66 (sept, $J_{H\text{-}H}$ = 6.8, 4H, C$\underline{H}$Me$_{IPr}$), 2.40, 2.27, 2.05 and 1.86 (all m, 8H, $CH_{2\text{-}cod}$), 1.42 and 1.23 (both d, $J_{H\text{-}H}$ = 6.8, 24H, Me$_{IPr}$). ^{13}C{^{1}H}-APT NMR (75 MHz, CD_2Cl_2, 298 K): δ 180.4 (d, $J_{C\text{-}Rh}$ = 77.2, CO), 173.5 (d, $J_{C\text{-}Rh}$ = 52.0, Rh-C$_{IPr}$), 145.7 (s, $C_{q\text{-}IPr}$), 134.2 (s, C_qN), 131.5 (s, $CH_{p\text{-}Ph}$), 126.7 (s, =CHN), 124.7 (s, $CH_{m\text{-}Ph}$), 114.1 (d, $J_{C\text{-}Rh}$ = 5.6, $CH_{cod\text{-}cis\text{-}IPr}$), 95.2 (d, $J_{C\text{-}Rh}$ = 6.7, $CH_{cod\text{-}trans\text{-}IPr}$), 30.0 and 29.8 (both s, $CH_{2\text{-}cod}$), 29.2 (s, C$\underline{H}$Me$_{IPr}$), 26.2 and 22.3 (both s, Me$_{IPr}$). ^{19}F NMR (282 MHz, CD_2Cl_2, 298 K): δ −73.1 (d, $J_{F\text{-}P}$ = 713.5, PF_6). ^{31}P NMR (121 MHz, CD_2Cl_2, 298 K): δ −144.6 (sept, $J_{P\text{-}F}$ = 713.5, PF_6).

Preparation of RhCl(CN^{t}Bu)$_2$(IPr) (9): A yellow solution of **3** (100 mg, 0.079 mmol) in 20 mL of tetrahydrofuran was treated with *tert*-butyl isocyanide (36 µl, 0.318 mmol) and it was stirred at room temperature for 30 min. Then, the solvent was evaporated to dryness, the solid product was dissolved in 10 mL of toluene and the solution was filtered through celite and the solvent was concentrated to ca. 1 mL. Addition of n-hexane induced the precipitation of a yellow solid, which was washed with n-hexane

(3×5 mL) and dried in vacuo. Yield: 67 mg (61%). Anal. Calcd. for $C_{37}H_{54}ClN_4Rh$: C, 64.11; H, 7.85; N, 8.08. Found: C, 64.02; H, 7.72; N, 8.15. IR (cm^{-1}, ATR): 2142 ν_a(CN), 2016 ν_s(CN). HRMS (ESI$^+$) *m/z* Calc for $RhC_{37}H_{55}N_4$ (M^+-Cl+H): 658.3476 Exp: 658.3452. ^{1}H NMR (400 MHz, C_6D_6, 298 K): δ 7.2–7.0 (6H, H_{Ph}), 6.70 (s, 2H, =CHN), 3.54 (sept, $J_{H\text{-}H}$=6.8, 4H, C<u>H</u>Me$_{IPr}$), 1.64 (d, $J_{H\text{-}H}$=6.8, 12H, Me$_{IPr\text{-}down}$), 1.11 (d, $J_{H\text{-}H}$=6.8, 12H, Me$_{IPr\text{-}up}$), 1.05 (s, 9H, ^{t}bu$_{\text{-}cis\text{-}IPr}$), 0.79 (s, 9H, tbu$_{\text{-}trans\text{-}IPr}$). ^{13}C{^{1}H}-APT NMR (100 MHz, C_6D_6, 298 K): δ 193.6 (d, $J_{C\text{-}Rh}$=45.0, Rh-C$_{IPr}$), 161.2 (d, $J_{C\text{-}Rh}$=71.8, Rh-C<u>N</u>C$_{cis\text{-}IPr}$), 150.4 (d, $J_{C\text{-}Rh}$=52.6, Rh-C<u>N</u>C$_{trans\text{-}IPr}$), 146.7 (s, C$_{q\text{-}IPr}$), 137.6 (s, C$_q$N), 129.6 (s, C$_{p\text{-}Ph}$), 124.0 (s, CH$_{m\text{-}Ph}$), 123.8 (s, =CHN), 55.9 (s, Rh-CN<u>C</u>$_{cis\text{-}IPr}$), 55.1 (s, Rh-CN<u>C</u>$_{trans\text{-}IPr}$), 31.3 (s, C(<u>C</u>H$_3$)$_{3\text{-}cis\text{-}IPr}$), 30.2 (s, C(<u>C</u>H$_3$)$_{3\text{-}trans\text{-}IPr}$), 28.9 (s, <u>C</u>HMe$_{IPr}$), 26.3 (s, Me$_{IPr\text{-}down}$), 23.9 (s, Me$_{IPr\text{-}up}$).

Preparation of RhCl(IPr){P(OCH$_3$)$_3$}$_2$ (10): This complex was prepared as described for **9** starting from **3** (100 mg, 0.079 mmol) and trimethyl phosphite (39 mg, 0.318 mmol) and obtained as a yellow solid. Yield: 84 mg (68%). Satisfactory elemental analysis could not be obtained. HRMS (ESI$^+$) *m/z* Calc for $RhC_{33}H_{54}N_2O_6P_2ClNa$ (M^+ + Na): 797.2093 Exp: 797.2080. ^{1}H NMR (400 MHz, C_6D_6, 298 K): δ 7.2 - 7.0 (6H, H_{Ph}), 6.60 (s, 2H, =CHN), 3.64 (sept, $J_{H\text{-}H}$=6.8, 2H, C<u>H</u>Me$_{IPr\text{-}cis\text{-}Cl}$), 3.48 (sept, $J_{H\text{-}H}$=6.7, 2H, C<u>H</u>Me$_{IPr\text{-}cis\text{-}P}$), 3.44 (d, $J_{H\text{-}H}$= 11.3, 9H, OCH$_{3\text{-}trans\text{-}IPr}$), 3.12 (d, $J_{H\text{-}H}$=11.7, 9H, OCH$_{3\text{-}cis\text{-}IPr}$), 1.59 (d, $J_{H\text{-}H}$=6.8, 6H, Me$_{IPr\text{-}cis\text{-}Cl\text{-}down}$), 1.34 (d, $J_{H\text{-}H}$=6.8, 6H, Me$_{IPr\text{-}cis\text{-}P\text{-}down}$), 1.00 (d, $J_{H\text{-}H}$=6.8, 6H, Me$_{IPr\text{-}cis\text{-}P\text{-}up}$), 0.97 (d, $J_{H\text{-}H}$=6.8, 6H, Me$_{IPr\text{-}cis\text{-}Cl\text{-}up}$). ^{13}C {^{1}H}-APT NMR (100 MHz, C_6D_6, 298 K): δ 192.1 (ddd, $J_{C\text{-}Rh}$=45.7, $J_{C\text{-}P}$= 167.4 and 12.6, Rh-C$_{IPr}$), 148.7 (s, C$_{q\text{-}IPr\text{-}cis\text{-}Cl}$), 145.3 (s, C$_{q\text{-}IPr\text{-}cis\text{-}P}$), 137.6 (s, C$_q$N), 129.1 (s, CH$_{p\text{-}Ph}$), 123.9 (s, CH$_{m\text{-}Ph\text{-}cis\text{-}Cl}$), 123.7 (s, =CHN), 122.8 (s, CH$_{m\text{-}IPr\text{-}cis\text{-}P}$), 51.5 (s, OCH$_{3}$$^{\text{-}}$$_{cis\text{-}IPr}$), 51.4 (s, OCH$_{3}$$^{\text{-}}$$_{trans\text{-}IPr}$), 29.0 (s, <u>C</u>HMe$_{IPr\text{-}cis\text{-}Cl}$), 27.7 (s, <u>C</u>HMe$_{IPr\text{-}cis\text{-}P}$), 26.6 (s, Me$_{IPr\text{-}cis\text{-}Cl\text{-}up}$), 26.4 (s, Me$_{IPr\text{-}cis\text{-}P\text{-}up}$), 23.4 (s, Me$_{IPr\text{-}cis\text{-}Cl\text{-}down}$), 22.9 (s, Me$_{IPr\text{-}cis\text{-}P\text{-}down}$). ^{31}P{^{1}H} NMR (121 MHz, C_6D_6, 298 K): δ 143.7 (dd, $J_{P\text{-}Rh}$=159.9, $J_{P\text{-}P}$=63.0, P-(OCH$_3$)$_{3\text{-}trans\text{-}IPr}$), 141.6 (dd, $J_{P\text{-}Rh}$=263.3, $J_{P\text{-}P}$=63.0, P(OCH$_3$)$_{3\text{-}cis\text{-}IPr}$).

Preparation of Rh(CN)(η^4-cod)(IPr) (11): An orange solution of **1** (350 mg, 0.551 mmol) in 20 mL of acetonitrile was treated with silver cyanide (74 mg, 0.553 mmol) and it was stirred at room temperature for 30 min in the absence of light. Then, the suspension was filtered through celite and the solvent was evaporated to dryness. The resulting solid was dissolved in 10 mL of dichloromethane, the mixture was filtered again and concentrated to ca. 1 mL. Addition of hexane induced the precipitation of a yellow solid, which was washed with hexane (3×5 mL) and dried in vacuo. Yield: 255 mg (73%). Anal. Calcd. for $C_{36}H_{48}N_3Rh$: C, 69.11; H, 7.73; N, 6.72. Found: C, 68.98; H, 7.60; N, 6.82. IR (cm^{-1}, ATR): 2101 ν(CN). HRMS (ESI$^+$) *m/z* Calc for $RhC_{36}H_{49}N_3$ (M^++H): 626.2981 Exp: 626.2987. $RhC_{35}H_{48}N_2$ (M^+-CN): 599.2872 Exp: 599.2866. ^{1}H NMR (300 MHz, toluene-d_8, 213 K): δ 7.4–6.9 (6H, H_{Ph}), 6.65 (s, 2H, =CHN), 4.91 (br, 2H, CH$_{cod\text{-}trans\text{-}IPr}$), 4.02 (br, 2H, CH$_{cod\text{-}cis\text{-}IPr}$), 3.97 and 2.33 (both sept, $J_{H\text{-}H}$=6.7, 4H, C<u>H</u>Me$_{IPr}$), 1.86, 1.20, 1.14, and 0.96 (all d, $J_{H\text{-}H}$=6.7, 24H, Me$_{IPr}$), 1.7–1.4 (8H, CH$_{2\text{-}cod}$). ^{13}C{^{1}H}-APT NMR (75 MHz, toluene-d_8, 213 K): δ 187.9 (d, $J_{C\text{-}Rh}$=52.6, Rh-C$_{IPr}$), 147.7 and 145.0 (both s, C$_{q\text{-}IPr}$), 138.8 (d, $J_{C\text{-}Rh}$=53.3, CN), 136.0 (s, C$_q$N), 130.0 (s, CH$_{p\text{-}Ph}$), 125.0 (s, =CHN), 122.6 (s, CH$_{m\text{-}Ph}$), 87.6 (d, $J_{C\text{-}Rh}$=7.3, CH$_{cod\text{-}trans\text{-}IPr}$), 84.0 (d, $J_{C\text{-}Rh}$=8.0, CH$_{cod\text{-}cis\text{-}IPr}$), 32.1, 30.9, 30.0, and 23.2 (all s, CH$_{2\text{-}cod}$), 28.8 and 28.7 (both s, <u>C</u>HMe$_{IPr}$), 26.9, 26.5, 24.0, and 22.0 (all s, Me$_{IPr}$).

Preparation of [Rh{1κ*C*,2κ*N*-(CN)}(CO)(IPr)]$_3$ (12): Carbon monoxide was bubbled through a yellow solution of **11** (100 mg, 0.159 mmol) in 20 mL of dichloromethane at room temperature for 10 min. The solution was concentrated to ca. 1 mL and hexane was added to induce the precipitation of a yellow solid, which was washed with hexane (3×5 mL) and dried in vacuo. Yield: 39 mg (40%). IR (cm^{-1}, ATR): 2128 ν(CN), 1954 ν(CO). Satisfactory elemental analysis could not be obtained. HRMS (ESI$^+$) *m/z* Calc for $RhC_{29}H_{37}N_3O$ (M^+/3+H): 546.2005 Exp: 546.1986. ^{1}H NMR (300 MHz, CD_2Cl_2, 298 K): δ 7.44 (t, $J_{H\text{-}H}$=7.7, 2H, H$_{p\text{-}IPr}$), 7.25 (d, $J_{H\text{-}H}$=7.7, 4H, H$_{m\text{-}IPr}$), 7.03 (s, 2H, =CHN), 2.75 (sept, $J_{H\text{-}H}$=6.7, 4H, C<u>H</u>Me$_{IPr}$), 1.19 (d, $J_{H\text{-}H}$=6.7, 12H, Me$_{IPr\text{-}down}$), 0.99 (d, $J_{H\text{-}H}$=6.7, 12H, Me$_{IPr\text{-}up}$). ^{13}C{^{1}H}-APT NMR (75 MHz, CD_2Cl_2, 298 K): δ 191.1 (d, $J_{C\text{-}Rh}$=75.0, CO), 187.9 (d, $J_{C\text{-}Rh}$=44.3, Rh-C$_{IPr}$), 156.5 (dd, $J_{C\text{-}Rh}$=45.4, 5.4, CN), 146.8 (s, C$_{q\text{-}IPr}$), 136.7 (s, C$_q$N), 129.9 (s, CH$_{p\text{-}IPr}$), 124.6 (s, =CHN), 124.2 (s, CH$_{m\text{-}IPr}$), 28.8 (s, <u>C</u>HMe$_{IPr}$), 26.4 (s, Me$_{IPr\text{-}up}$) and 23.4 (s, Me$_{IPr\text{-}down}$).

Standard Conditions for the Catalytic reactions. In a Schlenk flask, 0.02 mmol of catalyst was dissolved in 1 mL of DMA and 1 mL of methanol under argon. Then, 1 mmol of alkyne was added and the Schlenk flask was heated at 70 °C for 24 h with magnetic stirring. The resulting mixture was diluted with 10 mL of ethyl acetate and 20 mL of water were added. The organic layer was collected and the aqueous layer was extracted three times with ethyl acetate. The combined organic fractions were washed with brine, dried over Na_2SO_4, filtered, and carefully concentrated to remove volatile materials. The obtained crude material was analyzed by NMR. Conversion and selectivity was determined by integration of key resonances of phenylacetylene and the reaction products.

Crystal Structure Determination. Single crystals suitable for the X-ray diffraction studies were grown by slow diffusion of diethyl ether into saturated CH_2Cl_2 solutions (**4**, **5**, **7**, and **8**), or alternatively slow diffusion of hexane into saturated toluene solutions (**9**, **10**, **11** and **12**). X-ray diffraction data were collected at 100(2) K on a Bruker APEX SMART CCD diffractometer (**4**, **5**, **7–11**) or on a Bruker APEX-DUO SMART CCD diffractometer at 120(2) K (**12**), in both cases with graphite-monochromated Mo−Kα radiation (λ=0.71073 Å) using <1° ω rotations. Intensities were integrated and corrected for absorption effects with SAINT-PLUS[34] and SADABS[35] programs, both included in the APEX2 or APEX3 packages. The structures were solved by the Patterson method with SHELXS-97[36] and refined by full matrix least-squares on F^2 with SHELXL-2014,[37] under WinGX.[38]

Crystal data and structure refinement for 4. $C_{38}H_{46}F_6N_4OPRh$, 822.67 g·mol^{-1}, orthorhombic, $P2_12_12_1$, a=11.8846(7) Å, b=15.2171(9) Å, c=21.0976(13) Å, V=3815.5(4) Å^3, Z=4, D_{calc}=1.432 g/cm^3, μ=0.554 mm^{-1}, F(000)=1696, 0.190×0.180×0.120 mm^3, yellow prism, $\theta_{min}/\theta_{max}$ 1.931/28.750°, index ranges $-15\le h\le 16$, $-19\le k\le 20$, $-28\le l\le 27$, reflections collected/independent 48011/9333 [R(int)=0.0402], T_{max}/T_{min} 0.9064/0.8058, data/restraints/parameters 9333/0/ 468, GooF(F^2)=1.016, R_1=0.0260 [I>2·σ(I)], wR^2=0.0567 (all data), absolute structure parameter −0.025(8), largest diff. peak/hole 0.681/−0.346 e·Å^{-3}. CCDC deposit number 2079423.

Crystal data and structure refinement for 5. $C_{35}H_{49}Cl_2F_6N_4O_{1.50}PRh$, 868.56 g·mol^{-1}, monoclinic, $P2_1/c$, a=12.7138(9) Å, b=13.4129(10) Å, c=23.8836(17) Å, β=90.2720(10)°, V=4072.8(5) Å^3, Z=4, D_{calc}=1.416 g·cm^{-3}, μ=0.651 mm^{-1}, F(000)=1788, 0.370×0.150×0.090 mm^3, yellow prism, $\theta_{min}/\theta_{max}$ 1.602/26.372°, index ranges $-15\le h\le 15$, $-16\le k\le 16$, $-29\le l\le 29$, reflections collected/independent 42583/8307 [R(int)=0.0344], T_{max}/T_{min} 0.8839/0.7946, data/restraints/parameters 8307/28/577, GooF(F^2)=1.031, R_1=0.0469 [I>2·σ(I)], wR^2=0.1176 (all data), largest diff. peak/hole 1.049/−0.969 e·Å^{-3}. CCDC deposit number 2079448.

Crystal data and structure refinement for 7. $C_{37}H_{51}F_6N_3PRh$, 785.68 g·mol^{-1}, monoclinic, $P2_1/n$, a=16.0083(8) Å, b=12.2949(6) Å, c=20.2009(10) Å, β=111.7170(10)°, V=3693.7(3) Å^3, Z=4, D_{calc}=1.413 g·cm^{-3}, μ=0.566 mm^{-1}, F(000)=1632, 0.300×0.200h×0.160 mm^3, yellow prism, $\theta_{min}/\theta_{max}$ 1.980/28.691°, index ranges $-21\le h\le 21$, $-16\le k\le 16$, $-26\le l\le 26$, reflections collected/independent 69650/9067 [R(int)=0.0296], T_{max}/T_{min} 0.8749/0.7931, data/restraints/parameters 9067/0/442, GooF(F^2)=1.035, R_1=0.0265 [I>2·σ(I)], wR^2=0.0663 (all data), largest diff. peak/hole 0.601/−0.477 e·Å^{-3}. CCDC deposit number 2079426.

Crystal data and structure refinement for 8. $C_{36}H_{48}F_6N_2OPRh$, 772.64 g·mol^{-1}, monoclinic, $P2_1/n$, $a=16.2096(10)$ Å, $b=11.6899(7)$ Å, $c=20.2146(13)$ Å, $\beta=111.6700(10)°$, $V=3559.7(4)$ Å^3, $Z=4$, $D_{calc}=1.442$ g·cm^{-3}, $\mu=0.587$ mm^{-1}, F(000) = 1600, 0.300×0.240×0.100 mm^3, yellow prism, $\theta_{min}/\theta_{max}$ 2.021/28.621°, index ranges $-21\le h\le 21$, $-14\le k\le 15$, $-27\le l\le 27$, reflections collected/independent 30432/8392 [R(int) = 0.0374], T_{max}/T_{min} 0.8813/0.7687, data/restraints/parameters 8392/0/432, GooF(F^2) = 1.032, $R_1=0.0357$ [$I>2\cdot\sigma(I)$], $wR^2=0.0915$ (all data), largest diff. peak/hole 1.149/−0.612 e·Å^{-3}. CCDC deposit number 2079424.

Crystal data and structure refinement for 9. $C_{37}H_{54}ClN_4Rh$, 693.20 g·mol^{-1}, monoclinic, $P2_1/n$, $a=12.2685(9)$ Å, $b=16.1969(11)$ Å, $c=18.9743(13)$ Å, $\beta=103.0180(10)°$, $V=3673.5(4)$ Å^3, $Z=4$, $D_{calc}=1.253$ g·cm^{-3}, $\mu=0.567$ mm^{-1}, F(000) = 1464, 0.330×0.220×0.170 mm^3, yellow prism, $\theta_{min}/\theta_{max}$ 2.118/28.702°, index ranges $-16\le h\le 16$, $-21\le k\le 20$, $-25\le l\le 24$, reflections collected/independent 56203/9035 [R(int) = 0.0409], T_{max}/T_{min} 0.8644/0.7618, data/restraints/parameters 9035/30/433, GooF(F^2) = 1.072, $R_1=0.0289$ [$I>2\cdot\sigma(I)$], $wR^2=0.0664$ (all data), largest diff. peak/hole 0.560/−0.492 e·Å^{-3}. CCDC deposit number 2079427.

Crystal data and structure refinement for 10. $C_{66}H_{108}Cl_2N_4O_{12}P_4Rh_2$, 1550.16 g·mol^{-1}, monoclinic, $P2_1/c$, $a=18.4448(19)$ Å, $b=20.611(2)$ Å, $c=20.722(2)$ Å, $\beta=106.3440(10)°$, $V=7559.6(13)$ Å^3, $Z=4$, $D_{calc}=1.362$ g·cm^{-3}, $\mu=0.649$ mm^{-1}, F(000) = 3248, 0.220×0.175×0.140 mm^3, yellow prism, $\theta_{min}/\theta_{max}$ 1.150/28.665°, index ranges $-24\le h\le 24$, $-27\le k\le 27$, $-27\le l\le 27$, reflections collected/independent 120578/18435 [R(int) = 0.0563], T_{max}/T_{min} 0.8813/0.7314, data/restraints/parameters 18435/0/839, GooF(F^2) = 1.072, $R_1=0.0330$ [$I>2\cdot\sigma(I)$], $wR^2=0.0829$ (all data), largest diff. peak/hole 0.890/−0.990 e·Å^{-3}. CCDC deposit number 2079425.

Crystal data and structure refinement for 11. $C_{36}H_{48}N_3Rh$, 625.68 g·mol^{-1}, monoclinic, $P2_1/n$, $a=10.815(3)$ Å, $b=18.845(5)$ Å, $c=15.801(4)$ Å, $\beta=91.878(3)°$, $V=3218.7(15)$ Å^3, $Z=4$, $D_{calc}=1.291$ g·cm^{-3}, $\mu=0.558$ mm^{-1}, F(000) = 1320, 0.270×0.180×0.070 mm^3, yellow prism, $\theta_{min}/\theta_{max}$ 1.682/28.310°, index ranges $-14\le h\le 14$, $-25\le k\le 24$, $-21\le l\le 20$, reflections collected/independent 44439/7792 [R(int) = 0.0550], T_{max}/T_{min} 0.9143/0.7867, data/restraints/parameters 7792/0/369, GooF(F^2) = 1.049, $R_1=0.0331$ [$I>2\cdot\sigma(I)$], $wR^2=0.0703$ (all data), largest diff. peak/hole 0.614/−0.690 e·Å^{-3}. CCDC deposit number 2079429.

Crystal data and structure refinement for 12. $C_{96}H_{136}N_9O_3Rh_3$, 1722.72 g·mol^{-1}, triclinic, $P-1$, $a=15.246(4)$ Å, $b=16.376(4)$ Å, $c=19.993(5)$ Å, $\alpha=106.751(3)°$, $\beta=101.342(3)°$, $\gamma=98.562(4)°$, $V=4572.9(19)$ Å^3, $Z=2$, $D_{calc}=1.251$ g·cm^{-3}, $\mu=0.586$ mm^{-1}, F(000) = 1804, 0.150×0.120×0.030 mm^3, yellow prism, $\theta_{min}/\theta_{max}$ 1.099/25.028°, index ranges $-18\le h\le 18$, $-18\le k\le 19$, $-23\le l\le 23$, reflections collected/independent 36188/16140 [R(int) = 0.1008], T_{max}/T_{min} 0.9583/0.7674, data/restraints/parameters 16140/0/943, GooF(F^2) = 0.961, $R_1=0.0530$ [$I>2\cdot\sigma(I)$], $wR^2=0.1473$ (all data), largest diff. peak/hole 1.638/−1.192 e·Å^{-3}, CCDC deposit number 2079428.

Deposition Numbers 2079423 (for **4**), 2079448 (for **5**), 2079426 (for **7**), 2079424 (for **8**), 2079427 (for **9**), 2079425 (for **10**), 2079429 (for **11**), and 2079428 (for **12**) contain the supplementary crystallographic data for this paper. These data are provided free of charge by the joint Cambridge Crystallographic Data Centre and Fachinformationszentrum Karlsruhe Access Structures service www.ccdc.cam.ac.uk/structures.

Acknowledgements

Financial support from the Spanish Ministerio de Ciencia e Innovación (MICINN/FEDER) under the Project PID2019-103965GB–I00 and the Departamento de Ciencia, Universidad y Sociedad del Conocimiento del Gobierno de Aragón (group E42 20R) are gratefully acknowledged. A.D.G. thanks the Spanish Ministerio de Economía y Competitividad (MINECO) for the postdoctoral grant Juan de la Cierva - Incorporación2015 (IJCI-2015-27029).

Conflict of Interest

The authors declare no conflict of interest.

Keywords: N-Heterocyclic carbene · Rhodium · π-acceptor ligands · Hydroalkoxylation · Alkyne dimerization

[1] a) W. Hermann, *Angew. Chem. Int. Ed.* **2002**, *41*, 1290–1309; *Angew. Chem.* **2002**, *114*, 1342–1363; b) S. Díez-González, N. Marion, S. P. Nolan, *Chem. Rev.* **2009**, *109*, 3612–3676; c) D. J. Müller, C. Schlepphorst, F. Glorius, *Chem. Soc. Rev.* **2017**, *46*, 4845–4854; d) E. Peris, *Chem. Rev.* **2018**, *118*, 9988–10031; e) J. Lee, H. Hahm, J. Kwak, M. Kim, *Adv. Synth. Catal.* **2019**, *361*, 1479–1499; f) Q. Zhao, G. Meng, S. P. Nolan, M. Szostak, *Chem. Rev.* **2020**, *120*, 1981–2048.

[2] a) W. Hermann, *J. Organomet. Chem.* **1990**, *383*, 21–44; b) H. Werner, *Angew. Chem. Int. Ed.* **1990**, *29*, 1077–1089; *Angew. Chem.* **1990**, *102*, 1109–1121; c) Q. Xu, *Coord. Chem. Rev.* **2002**, *231*, 83–108; d) J. Bohnenberger, M. Schmitt, W. Feuerstein, I. Krummenacher, B. Butschke, J. Czajka, P. J. Malinowski, F. Breher, I. Krossing, *Chem. Sci.* **2020**, *11*, 3592–3603.

[3] a) P. Buchgraber, L. Toupet, V. Guerchais, *Organometallics* **2003**, *22*, 5144–5147; b) H. van Rensburg, R. P. Tooze, D. F. Foster, A. M. Z. Slawin, *Inorg. Chem.* **2004**, *43*, 2468–2470; c) J. Ruiz, G. García, M. E. G. Mosquera, B. F. Perandones, M. P. Gonzalo, M. Vivanco, *J. Am. Chem. Soc.* **2005**, *127*, 8584–8585; d) J. Cabeza, P. García-Alvarez, *Coord. Soc. Rev.* **2011**, *40*, 5389–5405; e) C. Dash, A. Das, M. Yousufuddin, H. V. R. Dias, *Inorg. Chem.* **2013**, *52*, 1584–1590; f) Z. Wang, L. Jiang, D. K. B. Mohamed, J. Zhao, T. S. A. Hor, *Coord. Soc. Rev.* **2015**, *293–294*, 292–326; g) P. V. Simpson, M. Falasca, M. Massi, *Chem. Commun.* **2018**, *54*, 12429–12438.

[4] a) V. Dragutan, I. Dragutan, L. Delaude, A. Demonceau, *Coord. Chem. Rev.* **2007**, *251*, 765–794; b) H. Li, L. C. M. Castro, J. Zheng, T. Roisnel, V. Dorcet, J.-B. Sortais, C. Darcel, *Angew. Chem. Int. Ed.* **2013**, *52*, 8045–8049; *Angew. Chem.* **2013**, *125*, 8203–8207; c) B. Saha, S. M. W. Rahaman, P. Daw, G. Sengupta, J. K. Bera, *Chem. Eur. J.* **2014**, *20*, 6543–6551; d) R. Lopes, B. Royo, *Isr. J. Chem.* **2017**, *57*, 1151–1159; e) F. Franco, M. F. Pinto, B. Royo, J. Lloret-Fillol, *Angew. Chem. Int. Ed.* **2018**, *57*, 4603–5606; *Angew. Chem.* **2018**, *130*, 4693–4696; f) R. Buhaibeh, C. Duhayon, D. A. Valyaev, J.-B. Sortais, Y. Canac, *Organometallics* **2021**, *40*, 231–241.

[5] a) Y. Canac, C. Lepetit, *Inorg. Chem.* **2017**, *56*, 667–675; b) H. V. Huynh, *Chem. Rev.* **2018**, *118*, 9457–9492.

[6] a) A. C. Chen, L. Ren, A. Decken, C. M. Crudden, *Organometallics* **2000**, *19*, 3459–3461; b) M. Bortenschlager, J. Schütz, D. von Preysing, O. Nuyken, W. A. Herrmann, R. Weberskirch, *J. Organomet. Chem.* **2005**, *690*, 6233–6237; c) J. M. Praetorius, M. W. Kotyk, J. D. Webb, R. Wang, C. M. Crudden, *Organometallics* **2007**, *26*, 1057–1061; d) W. Gil, K. Boczoń, A. M. Trzeciak, J. J. Ziółkowski, E. Garcia-Verdugo, S. V. Luis, V. Sans, *J. Mol. Catal. A* **2009**, *309*, 131–136; e) M. S. Jeletic, M. T. Jan, I. Ghiviriga, K. A. Abboud, A. S. Veige, *Dalton Trans.* **2009**, 2764–2776; f) A. R. Almeida, A. F. Peixoto, M. J. F. Calvete, P. M. P. Gois, M. M. Pereira, *Curr. Org. Chem.* **2011**, *8*, 764–775; g) D. Aucamp, T. Witteller, F. Dielmann, S. S. Siangwata, D. C. Liles, G. S. Smith, D. I. Bezuidenhout, *Eur. J. Inorg. Chem.* **2017**, 1227–1236; h) W. Alsalahi, A. M. Trzceiak, *Coord. Chem. Rev.* **2021**, *430*, 213732.

[7] a) S. Burling, L. D. Field, H. L. Li, B. A. Messerle, P. Turner, *Eur. J. Inorg. Chem.* **2003**, 3179–3184; b) M. Viciano, E. Mas-Marzá, M. Sanau, E. Peris, *Organometallics* **2006**, *25*, 3063–3069; c) M. L. Rosenberg, A. Krivokapic, M. Tilset, *Org. Lett.* **2009**, *11*, 547–550; d) J. Bexrud, M. Lautens, *Org. Lett.* **2010**, *12*, 3160–3163; e) G. Mancano, M. J. Page, M. Bhadbhade, B. A. Messerle, *Inorg. Chem.* **2014**, *53*, 10159–10170; f) V. Diachenko, M. J. Page, M. R. D. Gatus, M. Bhadbhade, B. A. Messerle, *Organometallics* **2015**, *34*, 4543–4552; g) L. Rubio-Pérez, M. Iglesias, J. Munarriz, V. Polo, J. J. Pérez-Torrente, L. A. Oro, *Chem. Eur. J.* **2015**, *53*, 17701–17707; h) A. Sarbajna, P. Pandey, S. M. W. Rahaman, K. Singh, A. Tyagi, P. H. Dixneuf, J. K. Bera, *ChemCatChem* **2017**, *9*, 1397–1401; i) C. M. Wong, M. B. Peterson, I. Pernik, R. T. McBurney, B. A. Messerle, *Inorg. Chem.* **2017**, *56*, 14682–14687; j) I. Strydom, G. Guisado-Barrios, I. Fernández, D. C. Liles, E. Peris, D. I. Bezuidenhout, *Chem. Eur. J.* **2017**, *23*, 1393–1401; k) L. Palacios, Y. Meheut, M. Galiana-Cameo, M. J. Artigas, A. Di Giuseppe, F. J. Lahoz, V. Polo, R. Castarlenas, J. J. Pérez-Torrente, L. A. Oro, *Organometallics* **2017**, *36*, 2198–2207.

[8] a) E. Singleton, H. E. Oosthuizen, *Adv. Organomet. Chem.* **1983**, *22*, 209–310; b) H. Werner, *Angew. Chem. Int. Ed. Engl.* **1990**, *29*, 1077–1089.

[9] a) C.-Y. Ho, T. F. Jamison, *Angew. Chem. Int. Ed.* **2007**, *46*, 782–785; *Angew. Chem.* **2007**, *119*, 796–799; b) M. Kim, T. Shin, A. Lee, H. Kim, *Organometallics* **2018**, *37*, 3253–3258; c) Y. D. Bidal, C. A. Urbina-Blanco, A. Poater, D. B. Cordes, A. M. Z. Slawin, L. Cavallo, C. S. J. Cazin, *Dalton Trans.* **2019**, *48*, 11326–11337; d) J. Duczynski, A. N. Sobolev, S. A. Moggach, R. Dorta, S. G. Stewart, *Organometallics* **2020**, *39*, 105–115.

[10] a) W. P. Fehlhammer, M. Fritz, *Chem. Rev.* **1993**, *93*, 1243–1280; b) M. Ohba, H. Okawa, *Coord. Chem. Rev.* **2000**, *198*, 313–328; c) J. R. Berenguer, J. Fernandez, E. Lalinde, S. Sánchez, *Organometallics* **2013**, *32*, 835–845.

[11] a) A. Di Giuseppe, R. Castarlenas, J. J. Pérez-Torrente, F. J. Lahoz, V. Polo, L. A. Oro, *Angew. Chem. Int. Ed.* **2011**, *50*, 3938–3942; *Angew. Chem.* **2011**, *123*, 4024–4028; b) A. Di Giuseppe, R. Castarlenas, J. J. Pérez-Torrente, M. Crucianelli, V. Polo, R. Sancho, F. J. Lahoz, L. A. Oro, *J. Am. Chem. Soc.* **2012**, *134*, 8171–8183; c) L. Rubio-Pérez, R. Azpíroz, A. Di Giuseppe, V. Polo, R. Castarlenas, J. J. Pérez-Torrente, L. A. Oro, *Chem. Eur. J.* **2013**, *19*, 15304–15314; d) R. Azpíroz, L. Rubio-Pérez, A. Di Giuseppe, V. Passarelli, F. J. Lahoz, R. Castarlenas, J. J. Pérez-Torrente, L. A. Oro, *ACS Catal.* **2014**, *4*, 4244–4253; e) A. Di Giuseppe, R. De Luca, R. Castarlenas, J. J. Pérez-Torrente, M. Crucianelli, L. A. Oro, *Chem. Commun.* **2016**, *52*, 5554–5557; f) R. Azpíroz, A. Di Giuseppe, V. Passarelli, J. J. Pérez-Torrente, L. A. Oro, R. Castarlenas *Organometallics* **2018**, *37*, 1695–1707; g) R. Azpíroz, A. Di Giuseppe, A. Urriolabeitia, V. Passarelli, V. Polo, J. J. Pérez-Torrente, L. A. Oro, R. Castarlenas, *ACS Catal.* **2019**, *9*, 9372–9386; h) M. Galiana-Cameo, M. Borraz, Y. Zelenkova, V. Passarelli, F. J. Lahoz, J. J. Pérez-Torrente, L. A. Oro, A. Di Giuseppe, R. Castarlenas, *Chem. Eur. J.* **2020**, *26*, 9598–9608.

[12] a) A. Di Giuseppe, R. Castarlenas, J. J. Pérez-Torrente, F. J. Lahoz, L. A. Oro, *Chem. Eur. J.* **2014**, *20*, 8391–8403; b) L. Palacios, A. Di Giuseppe, M. J. Artigas, V. Polo, F. J. Lahoz, R. Castarlenas, J. J. Pérez-Torrente, L. A. Oro, *Catal. Sci. Technol.* **2016**, *6*, 8548–8561; c) M. Galiana-Cameo, A. Urriolabeitia, E. Barrenas, V. Passarelli, J. J. Pérez-Torrente, A. Di Giuseppe, V. Polo, R. Castarlenas, *ACS Catal.* **2021**, *11*, 7553–7557.

[13] a) X.-Y. Yu, B. O. Patrick, B. R. James, *Organometallics* **2006**, *25*, 2359–2363; b) X.-Y. Yu, B. O. Patrick, B. R. James, *Organometallics* **2006**, *25*, 4870–4877; c) X.-Y. Yu, H. Sun, B. O. Patrick, B. R. James, *Eur. J. Inorg. Chem.* **2009**, 1752–1758.

[14] a) J. M. Praetorius, R. Wang, C. M. Crudden, *Eur. J. Inorg. Chem.* **2009**, 1746–1751; b) O. V. Zenkina, E. C. Keske, R. Wang, C. M. Crudden, *Organometallics* **2011**, *30*, 6423–6432; c) O. V. Zenkina, E. C. Keske, G. S. Kochhar, R. Wang, C. M. Crudden, *Dalton Trans.* **2013**, *42*, 2282–2293; d) E. C. Keske, O. V. Zenkina, A. Asadi, H. Sun, J. M. Praetorius, D. P. Allen, D. Covelli, B. O. Patrick, R. Wang, P. Kennepohl, B. R. James, C. M. Crudden, *Dalton Trans.* **2013**, *42*, 7414–7236.

[15] a) L. Palacios, A. Di Giuseppe, A. Opalinska, R. Castarlenas, J. J. Pérez-Torrente, F. J. Lahoz, L. A. Oro, *Organometallics* **2013**, *32*, 2768–2774; b) L. Palacios, A. Di Giuseppe, R. Castarlenas, F. J. Lahoz, J. J. Pérez-Torrente, L. A. Oro, *Dalton Trans.* **2015**, *44*, 5777–5789.

[16] a) A. Nevelling, G. R. Julius, S. Cronje, C. Esterhuysen, H. G. Raubenheimer, *Dalton Trans.* **2005**, 181–192; b) A. Bittermann, E. Herdtweck, P. Härter, W. A. Herrmann, *Organometallics* **2009**, *28*, 6963–6968; c) H. Buhl, C. Ganter, *J. Organomet. Chem.* **2016**, *809*, 74–78.

[17] a) B. E. Mann, *Organometallics* **2012**, *31*, 5728–5735; b) S. H. Heinemann, T. Hoshi, M. Westerhausen, A. Schiller, *Chem. Commun.* **2014**, *50*, 3644–3660.

[18] a) N. Tsoureas, A. A. Danopoulos, A. A. D. Tulloch, M. E. Light, *Organometallics* **2003**, *22*, 4750–4758; b) J. Langer, D. Walther, H. Görls, *J. Organomet. Chem.* **2006**, *691*, 4874–4881; c) J. Fawcett, D. A. J. Harding, E. G. Hope, K. Singh, G. A. Solan, *Dalton Trans.* **2010**, *39*, 10781–10789; d) S. Fuertes, A. J. Checa, V. Sicilia, *Inorg. Chem.* **2015**, *54*, 9885–9895.

[19] See this example for palladium: C.-C. Ho, S. Chatterjee, T.-L. Wu, K.-T. Chan, Y.-W. Chang, T.-H. Hsiao, H. M. Lee, *Organometallics* **2009**, *28*, 2837–2847.

[20] M. Brandl, S. Weiss, A. Jabs, J. Sühnel, R. Hilgenfelf, *J. Mol. Biol.* **2001**, *307*, 357–377.

[21] For comparison of ^{13}C metal-carbene chemical shift for neutral and cationic Rh–NHC–CO derivatives see: E. L. Kolychev, S. Kronig, K. Brandhorst, M. Freytag, P. G. Jones, M. Tamm, *J. Am. Chem. Soc.* **2013**, *135*, 12448–12459.

[22] Inertness of a Rh–NHC-cod complex towards CO bubbling has been reported: A. Magriz, S. Gómez-Bujedo, E. Álvarez, R. Fernández, J. M. Lasaletta, *Organometallics* **2010**, *29*, 5941–5945.

[23] A cationic Rh–CO-cod complex bearing a Fisher carbene has been prepared by CO transmetallation: J. Barluenga, R. Vicente, L. A. López, E. Rubio, M. Tomás, C. Álvarez-Rúa, *J. Am. Chem. Soc.* **2004**, *126*, 470–471.

[24] a) C. S. Chin, B. Lee, S. Kim, *Organometallics* **1993**, *12*, 1462–1466; b) L. D. Field, B. A. Messerle, K. Q. Vuong, P. Turner, *Organometallics* **2005**, *24*, 4241–4250.

[25] a) S. McGrandle, G. C. Saunders, *J. Fluorine Chem.* **2005**, *126*, 451–455; b) S. Xu, K. Manna, A. Ellern, A. D. Sadow, *Organometallics* **2014**, *33*, 6840–6860.

[26] a) C.-Y. Wang, Y.-H. Liu, S.-M. Peng, S.-T. Liu, *J. Organomet. Chem.* **2006**, *691*, 4012–4020; b) W. Gil, A. M. Trzeciak, J. J. Ziolkowski, *Organometallics* **2008**, *27*, 4131–4138.

[27] a) W. C. Kalb, Z. Demidowicz, D. M. Speckman, C. Knobler, R. G. Teller, F. Hawthorne, *Inorg. Chem.* **1982**, *21*, 4027–4036; b) K. K. Klausmeyer, Thomas, B. Rauchfuss, S. R. Wilson, *Angew. Chem. Int. Ed.* **1998**, *37*, 1694–1696; *Angew. Chem.* **1998**, *110*, 1808–1810; c) M. L. Kuhlman, T. B. Rauchfuss, *J. Am. Chem. Soc.* **2003**, *125*, 10084–1092; d) A. Rodriguez, H. Sakiyama, N. Masciocchi, S. Galli, N. Gálvez, F. Lloret, E. Colacio, *Inorg. Chem.* **2005**, *44*, 8399–8406.

[28] a) S. Paziresh, V. Sicilia, I. Ara, A. Martín, S. Fuertes, *Organometallics* **2019**, *38*, 3804–3815; b) D. Saito, T. Ogawa, M. Yoshida, J. Takayama, S. Hiura, A. Murayama, A. Kobayashi, M. Kato, *Angew. Chem. Int. Ed.* **2020**; *59*, 18723–18730.

[29] M. Angoy, M. V. Jiménez, P. García-Orduña, L. A. Oro, E. Vispe, J. J. Pérez-Torrente, *Organometallics* **2019**, *38*, 1991–2006.

[30] O. Torres, M. Fernàndez, A. Diáz-Jiménez, A. Pla-Quintana, A. Roglans, M. Solà, *Organometallics* **2019**, *38*, 2853–2862.

[31] a) B. M. Trost, M. T. Rudd, *J. Am. Chem. Soc.* **2003**, *125*, 11516–11517; b) K. Tanaka, S. Saitoh, H. Hara, Y. Shibata, *Org. Biomol. Chem.* **2009**, *7*, 4817–4820; c) Y. Minami, Y. Noguchi, M. Yamada, C. Tsuruoka, Y. Furuya, T. Hiyama, *Chem. Lett.* **2018**, *47*, 1288–1291.

[32] a) M. Kondo, T. Kochi, F. Kakiuchi, *J. Am. Chem. Soc.* **2011**, *133*, 32–34; b) F. Kakiuchi, S. Takano, T. Kochi, *ACS Catal.* **2018**, *8*, 6127–6137.

[33] Y. Morimoto, M. Hamada, S. Takano, K. Mochizuki, T. Kochi, F. Kakiuchi, *Org. Lett.* **2021**, *23*, 3803–3808.

[34] *SAINT+: Area-Detector Integration Software*, version 6.01; Bruker AXS: Madison, WI, **2001**.

[35] G. M. Sheldrick, *SADABS program*; University of Göttingen: Göttingen, Germany, **1999**.

[36] G. M. Sheldrick, *SHELXS 97*, University of Göttingen: Göttingen, Germany, **1997**.

[37] G. M. Sheldrick, *Acta Crystallogr. Sect. C* **2015**, *71*, 3–8.

[38] L. J. Farrugia, *J. Appl. Crystallogr.* **2012**, *45*, 849–854.

Manuscript received: May 10, 2021
Revised manuscript received: June 9, 2021
Accepted manuscript online: June 10, 2021